

ALMA MATER STUDIORUM - UNIVERSITÀ DI BOLOGNA

---

SCUOLA DI INGEGNERIA E ARCHITETTURA

*DIPARTIMENTO DI INGEGNERIA INDUSTRIALE - DIN*

*CORSO DI LAUREA MAGISTRALE IN INGEGNERIA MECCANICA*

TESI DI LAUREA

in

Meccanica delle Macchine M

DYNAMIC MODELLING AND SIMULATION OF A  
CABLE-DRIVEN PARALLEL ROBOT FOR  
REHABILITATION APPLICATIONS

CANDIDATO:  
Enrico Sammarchi

RELATORE:  
Prof. Ing. Marco Carricato

CORRELATORI:  
Ing. Edoardo Idà  
Prof. Ing. Sunil K. Agrawal  
Ing. Moitz Khan

Anno accademico 2017/2018

Sessione III



# Abstract

In the last years, rehabilitation robotics has had a great development in the medical field and research centers of all over the World find every day new challenges and solutions for the improvement of physical and psychological life of people. Cable-driven parallel robots have earned a fundamental role for this aim, and they are applied more and more as rehabilitation robotic devices.

The aim of this work, in collaboration with the ROAR Lab of the Columbia University in the city of New York, is to build a simulation model of a new cable-driven parallel robot for rehabilitation applications, being able to compute the effort given by the patient while the system is working on him/her. The developed model was built on a multi-body dynamic software called *Adams*, which is able to simulate the behavior of several mechanisms.

In this thesis, some theoretical issues about cable-driven parallel robots will be introduced first, in order to familiarize with the application and introduce the state of the art of the topic. General foundations, dealing with kinematics, statics, dynamics will be detailed and a short introduction to control will be given.

In the second chapter, a brief overview of the state of the art regarding rehabilitation cable-driven robotics will be outlined, first dealing with general applications possible to be found in literature, and then introducing the Columbia University work about this particular topic, with several examples and cutting edge devices.

The third chapter is about the design description of the Stand Trainer, a 8-cable-driven parallel robot used for rehabilitation developed by the Columbia University ROAR Lab. Its mechanical system is introduced, while dealing especially with the issue of computing the cable tensions and the way it can be done in terms of sensors positioning. A new way of cable tension measurement will be explained and its advantages outlined.

The last chapter deals with the dynamic simulations on Adams. After having introduced all the simplifications regarding three different Adams models of the robot, an accurate description of them will be given and their comparison with the real device will be outlined. The post-process activity will be carried out explaining and discussing the final results, after having chosen the model that better represents the real device.

Finally, different points for future developments will be discussed, showing the novelty of this approach for rehabilitative treatments and applications.



# Contents

<b>1</b>	<b>Cable Driven Parallel Robots - Theory Foundations</b>	<b>7</b>
1.1	Standard Geometric Model . . . . .	7
1.2	Description of Geometry and Kinematic Model . . . . .	9
1.3	Statics . . . . .	10
1.4	Dynamics . . . . .	14
<b>2</b>	<b>Rehabilitation with Cable Driven Parallel Robots</b>	<b>17</b>
2.1	Literature Overview . . . . .	17
2.2	The Columbia University Activity . . . . .	22
2.2.1	TruSt: Trunk Support Trainer . . . . .	23
2.2.2	TPAD: Tethered Pelvic Assist Device . . . . .	24
2.2.3	C-ALEX: Cable-driven Active Leg Exoskeleton . . . . .	25
2.2.4	CAREX: Cable-Driven Arm Exoskeleton . . . . .	27
<b>3</b>	<b>The Stand Trainer</b>	<b>31</b>
3.1	Description of the Robot . . . . .	31
3.1.1	The Mechanical System . . . . .	31
3.1.2	The Control System . . . . .	36
3.2	Cable Tension Measurement . . . . .	37
3.2.1	A New Way of Cable Tension Monitoring . . . . .	38
3.2.1.1	Tests for the Correlation . . . . .	41
<b>4</b>	<b>Adams Simulations</b>	<b>49</b>
4.1	Introduction to the software . . . . .	49
4.1.1	Simplified Method . . . . .	50
4.1.2	Discretized Method . . . . .	51
4.2	The Stand Trainer Models . . . . .	52
4.2.1	Model 1: application of the motors velocities . . . . .	53
4.2.1.1	Model 1 Outputs . . . . .	55
4.2.2	Model 2: application of the cable tensions . . . . .	57
4.2.2.1	Model 2 Outputs . . . . .	59
4.2.3	Model 3: application of the cable tensions and the motion to the belt COM . . . . .	59
4.3	Post-Processing and Results . . . . .	62
4.3.1	Force Control in Rehabilitation . . . . .	62
4.3.2	Post-Processing of the Model . . . . .	63
4.3.3	Model Limitations . . . . .	68

<b>5</b>	<b>Conclusions</b>	<b>71</b>
5.1	Discussion of the Results . . . . .	71
5.2	Future Developments . . . . .	72

# Chapter 1

## Cable Driven Parallel Robots - Theory Foundations

Most of the theoretical concepts explained in this chapter takes inspiration from the works [3], [9] and [20]. Cable Driven Parallel Robots (CDPRs) are particular types of Parallel Manipulators where the members that connect the frame to the end-effector are not rigid links, but simple cables. Since they can only work in traction, they only admit pulling forces, and because of that, controlling a CDPR may be harder than a usual rigid-link parallel mechanism.

These types of manipulators are suitable for high speed tasks, since their mechanical components (i.e. the cables) are lightweight, but they are also able to move high payloads. In fact, the first CDPRs that have been conceived were used as cranes, machines that can lift very heavy loads and, at the same time, keep a high load to weight ratio. Only in a second moment they started to be used in different fields for different tasks, like the medical ones.

The evolution of these mechanisms is pretty recent: only in the last 30-40 years there has been an evolution of this topic, solving most of the kinematic and static problems. Despite the large steps taken in the last years, some issues remain unsolved, but evolution of technology is helping, finding new challenges and scientific results that allow for their development.

### 1.1 Standard Geometric Model

The figure 1.1 shows the main parts a cable robot is composed by, underlining their terminology.

In order to have a first approach to the problem, it is necessary to introduce a simplified model of the robot able to describe its behavior in a less complex way, instead of considering all the occurring effects present in the real model. In literature, this goes under the name of Standard Geometric Model, also called Standard Model. In the Standard Model, the cables are idealized as exact linear distance between two points in space, i.e. the proximal anchor point on the fixed frame and the distal anchor point on the mobile platform. Thus, it is assumed that the cable length matches exactly this distance. In the terms of multi-body systems, cables are modeled to be prismatic joints. Both ends of the cables are modeled by spherical joints. To better understand the behavior of CDPRs, this simplified model can be considered: using these simplifications some real effects will be neglected.

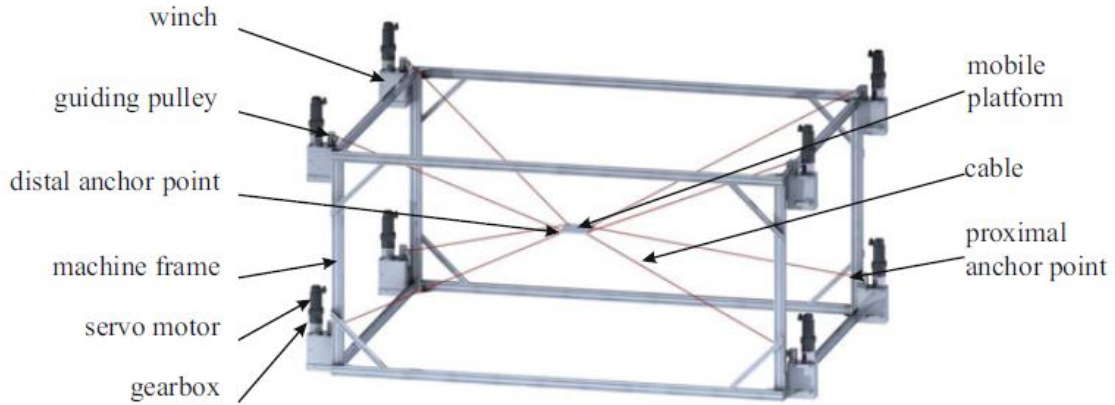


Figure 1.1: General terminology when talking about cable-driven parallel robots.

The *Simplified Geometric Model* affects the following parameters that can be met while handling with CDPRs:

- *Unilateral constraint*: the cables can only pull, not push, so the constraint equations will have inequalities instead of equalities, that will make the algebraic system more difficult to solve;
- *Elastic Cables*: the deformation of the cable is neglected, therefore it's supposed that the length of the cable will remain the same if the pulley where the cable is coiled on doesn't roll;
- *Temperature Effects*: the temperature of the cables can rise while the system is working, but this effect is neglected;
- *Undefined Cable Guidance*: the cable can be coiled in a unpredictable way around the drum, affecting its effective length;
- *Nontrivial winch and platform kinematics*: the model is considered having spherical joints to the anchor points, and a prismatic joint along the cable. These assumption could not be perfectly true due the fact that the effective length of the cable may depend on its actual direction with respect to the winch, on the orientation of the platform;
- *Hefty Cables*: cables are thought as massless elements. Actually, due to their mass, cables are subject to sagging and get a curved shape which can significantly differ from the straight line of the standard model. This must be taken into account while modeling large-scale cable robots with very long cables, relatively heavy, kept under low tension, or when high accuracy of the robot shall be achieved;
- *Creeping and Hysteresis Effects*: this phenomenon is not taken into account, but in reality these effects occur in the cables depending on the material and the type. Changing in length can occur with cables under tension and the material could tend to age and be subject to wear in a more significant way;
- *Vibration of the Cable*: this effect is neglected by the model, but longitudinal and transversal vibrations can occur when the system is operating, mainly for



large-scale robots, where the cables are larger and tend to vibrate more. It can happen when there are changes in cable tension;

- *Coiling the cable with varying tension onto a drum*: there could be some errors when coiling cables around the drums due to their ovalization, therefore the coiling radius will change and some changes in length will occur due to hysteresis effects;
- *Elastic Reactions of the Mobile Platform*: constraints are modeled rigid, even if there is a little deformation due to the tension applied to the cables by the motors. The higher the loads are and the less stiff the frame is, the higher the deformation of the frame will be.

Differently from the other types of parallel manipulators, CDPRs have the feature that Kinematics and Statics are joined, reason why in order to completely know the system parameters, it is necessary to solve both. This is one of the reasons why CDPRs are complex mechanisms.

## 1.2 Description of Geometry and Kinematic Model

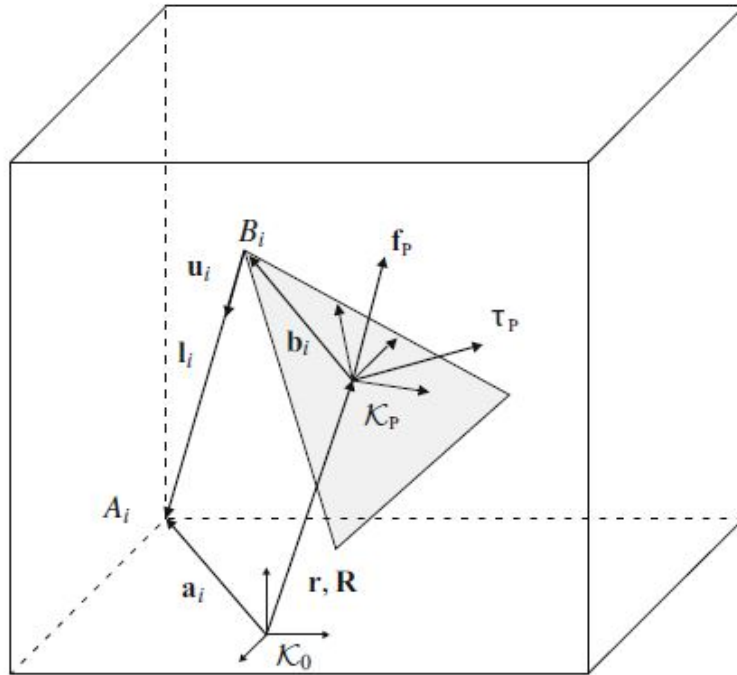


Figure 1.2: General approach for geometry and kinematics for a CDPR

By considering figure 1.2 it is possible to derive the general geometric model of a CDPR, with which it will be possible to describe its Kinematics. Also, it puts the foundations to describe both Statics and Dynamics of the robot.

The reference coordinates systems are  $K_0$ , attached to the frame, and  $K_P$ , attached to the platform. The anchor points attached to the frame are called  $A_i$ , while those attached to the moving platform are called  $B_i$ . In general, one cannot say that the

number of anchor points is equal to the number of cables because, in some cases, some cables could share the same anchor. Position vectors  $\mathbf{a}_i$  denote the proximal attachment points  $A_i$  on the frame in world coordinates  $K_0$ , whereas vectors  $\mathbf{b}_i$  are the positions of the distal attachment points  $B_i$  on the mobile platform relative to the origin of  $K_P$  given in local coordinates of the frame  $K_P$ , and  $\mathbf{l}_i$  denotes the vector of the cable lengths in  $K_0$ .

In this model, it is assumed that cable lengths are simply the distances between the anchor points  $A_i$  and  $B_i$ , so they are thought as straight lines under tension; moreover, vectors  $\mathbf{a}_i$  and  $\mathbf{b}_i$  do not depend from the pose of the platform.

Finally, the position of the platform with respect to the reference frame is indicated with  $\mathbf{r}$ .

By considering the geometry of the model, it's now possible to write the closure equation of the mechanism:

$$\mathbf{a}_i - \mathbf{r} - \mathbf{R}\mathbf{b}_i - \mathbf{l}_i = \mathbf{0}; \text{ for } i = 1, \dots, m; \quad (1.1)$$

where  $\mathbf{R}$  is the rotational matrix that transforms the coordinates of a vector with respect to  $K_P$  in the coordinates of the same vector with respect to  $K_0$ .

The couple  $(\mathbf{R}, \mathbf{r})$  describes the pose of the platform with respect to the frame, which means that it transforms the coordinates system from  $K_P$  to  $K_0$ .

It can be useful to indicate the unit vector that identifies the direction of the cable. Using equation 1.1 it's possible to derive the length  $l_i$  that the cable is supposed to have

$$\mathbf{l}_i = \mathbf{a}_i - \mathbf{r} - \mathbf{R}\mathbf{b}_i; \text{ for } i = 1, \dots, m; \quad (1.2)$$

and then derive the unit vector  $u_i$ : it points from the platform to the base, as it is possible to see from the 1.1, and it can be written as:

$$\mathbf{u}_i = \frac{\mathbf{l}_i}{\|\mathbf{l}_i\|_2}; \text{ for } i = 1, \dots, m; \quad (1.3)$$

The analysis described above is purely geometric and nothing was said concerning the ability of the mechanism to maintain tension in the cables. This issue will be faced in the next section.

### 1.3 Statics

It is mandatory to solve the static problem for CDPRs in order to control the mechanism either in position or in force. The knowledge of the kinematic properties is not enough, due to the fact that cables, contrary to the rigid links that other parallel mechanisms own, can not provide pushing loads, but they can only pull.

Therefore, the static analysis should be joined with the Kinematic one described above.

Equilibrium equations for forces and torques acting on the system can be written as:

$$\sum_{i=1}^m \mathbf{f}_i + \mathbf{f}_p = \mathbf{0} \quad (1.4)$$

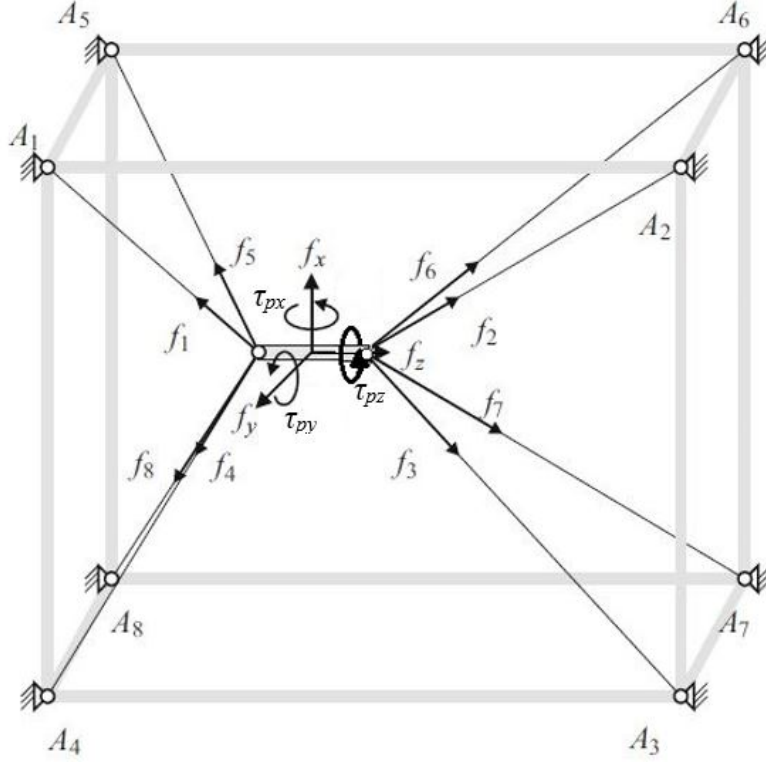


Figure 1.3: Scheme of the CDPR statics.

$$\sum_{i=1}^m (\mathbf{b}_i \times \mathbf{f}_i) + \boldsymbol{\tau}_p = \mathbf{0} \quad (1.5)$$

where  $\mathbf{f}_p$  and  $\boldsymbol{\tau}_p$  are the vectors of external forces and torques applied to the mobile platform center of mass, respectively, while  $\mathbf{f}_i$  is the force vector that each cable applies on the end-effector (figure 1.3).

By the knowledge of the cables direction, as the unit vectors  $\mathbf{u}_i$  are known, the direction of the forces  $\mathbf{f}_i$  are also known, leading to the relation:

$$\mathbf{f}_i = f_i \mathbf{u}_i \quad (1.6)$$

This equation is a key relationship in the kinematics, statics and dynamics of CD-PRs. It is possible to rewrite the equations 1.4 and 1.5 in matrix form, leading to a more compact way to mathematically represent the problem:

$$\begin{bmatrix} \mathbf{u}_1 & \cdots & \mathbf{u}_m \\ \mathbf{b}_1 \times \mathbf{u}_1 & \cdots & \mathbf{b}_m \times \mathbf{u}_m \end{bmatrix} \begin{bmatrix} f_1 \\ \vdots \\ f_m \end{bmatrix} + \begin{bmatrix} \mathbf{f}_p \\ \boldsymbol{\tau}_p \end{bmatrix} = \mathbf{0} \quad (1.7)$$

By defining:

$$\mathbf{A}^T = \begin{bmatrix} \mathbf{u}_1 & \cdots & \mathbf{u}_m \\ \mathbf{b}_1 \times \mathbf{u}_1 & \cdots & \mathbf{b}_m \times \mathbf{u}_m \end{bmatrix} \quad (1.8)$$

$$\mathbf{w}_p = \begin{bmatrix} \mathbf{f}_p \\ \boldsymbol{\tau}_p \end{bmatrix} \quad (1.9)$$

it's possible to rewrite the equation 1.7 as:

$$\mathbf{A}^T \mathbf{f} + \mathbf{w}_p = \mathbf{0} \quad (1.10)$$

The following terms can be identified:

- $\mathbf{f}$ : vector of the cables tensions ( $m \times 1$ );
- $\mathbf{A}$ : Jacobian matrix of the system, it transforms cable forces from the joint space into the end-effector Cartesian wrench in the operational space ( $n \times m$ );
- $\mathbf{w}_p$ : vector of the external wrenches applied on the mobile platform center of mass ( $n \times 1$ );

What can be pointed out, for instance, is that, under static conditions, the platform wrench  $\mathbf{w}_p$  represents the wrench induced by gravity on the platform, if no other load is applied to it. If one considered Dynamics too, the vector  $\mathbf{w}_p$  would represent the wrench induced by gravity plus the inertial effects associated with the platform motion.

By considering equation 1.10, it is pretty simple to distinguish some cases which can occur while dealing with the problem of cable robots. Controlling the robot with force control, cable forces  $\mathbf{f}$  are considered unknown, because the Cartesian wrench applied to the end-effector is imposed by the user, but cable tensions follow the robot geometry. Alternatively, while dealing with a motion control, the Cartesian position of the end-effector is imposed, therefore cable vectors must be computed applying the Jacobian of the system. The equation system 1.10 has  $m$  unknowns and a number of equations (constraints) equals to  $n$ . Depending on the degree of redundancy  $r = m - n$ , it is possible to distinguish three different cases, which characterize the CDPR:

- $r < 0$ : The number of equation is greater than the number of unknowns, that means there are more constraints than degrees of freedom (DOFs), therefore the system results over-determined and the robot itself under-actuated. Basically there are less cables than available platform DOFs. CDPRs like this are called *Incompletely Restrained Positioning Mechanisms* (IRPM) and they rely to external forces (for instance, gravity) in order to work properly and maintain their stability;
- $r = 0$ : the number of unknowns is the same as the number of equations, that means the system is completely determined and its solution is unique. These robots also belong to the IRPM class since they rely on the external forces;
- $r > 0$ : the number of unknowns is greater than the number of equations, it means that the problem is under-determined and the robot is over-constrained. There are more cables than available DOFs of the platform. In this case, there exist infinite number of solutions. There are some methods that add some equations in relation to the value of  $r$  and to the task one wants to perform. In this case, it is possible to distinguish two subclasses of them:
  - *Completely Restrained Positioning Mechanisms* (CRPM): for these CDPRs it holds  $m = n + 1$ ;

- *Redundantly Restrained Positioning Mechanisms* (RRPM): for these CD-PRs it holds  $m > n + 1$ .

Most of the CDPRs are built in this way, because it is easier to control the end-effector, and the system results more stiff, since there are more cables that constraint its position.

When dealing with problems where cable tensions are already known and the external wrench has to be determined, the equation 1.10 become simply an algebraic equation that can be trivially solved:

$$\mathbf{w}_p = -\mathbf{A}^T \mathbf{f} \quad (1.11)$$

As it was pointed out before, contrary to the other rigid parallel mechanisms, the nature of cables as unilateral constraint allows them only to be pulled, that means considering only a subset of the solutions set one can find solving the system. This subset is the one where all the cable forces are supposed to be positive ( $f_i > 0$ ).

This unilateral nature of the problem makes it trickier than the normal and the methods that can be used to solve it are different from the usual algorithms, because as said they have to guarantee the positivity of the cable forces.

In literature, it is possible to find many different algorithms that allow to solve this particular problem. Most of them are thought to solve RRPM and CRPM, where the problem is *under-determined* and the robot is *over-constrained*.

Here, an overview of the most important methods able to solve the system 1.10 and to compute cable force distribution for CRPM cable robots:

- Linear Programming;
- Nonlinear Programming;
- Verhoeven's Gradient Method;
- Dykstra Method;
- Closed-Form Method and improvements;
- Barycentric Force Distribution Method;
- Weighted Sums of Vertices;
- Puncture method.

Some of them are more feasible for real-time control, while others are better to find initial conditions for the integration of the entire solution. In some cases, one can also use a combination of them to control the device and to reach a better estimation of the solution.

## 1.4 Dynamics

Since it has been pointed out that CDPRs have the advantage to move high loads at a high speed thanks to the properties of lightness and flexibility of the cables, it is worth considering not only statics, but also dynamics, that is, the study of the system equilibrium during the motion. In fact, in the computation of the forces acting on the platform, it is necessary to add its inertia actions, i.e. it is necessary to include them in the computation of  $\mathbf{w}_p$ , which is not negligible when considering the Dynamics, especially when using big cable robots, where the end effector is heavy and the inertia actions become more important.

Basically, the equilibrium equations discussed in the previous section remain the same, with the difference that the inertia of the end-effector has to be added on the right side of it. Respectively, the following equations show the equilibrium for translations and rotations:

$$m\ddot{\mathbf{r}} = \mathbf{f}_p + \mathbf{f}_{\text{cable}} \quad (1.12)$$

$$\mathbf{I}\dot{\boldsymbol{\omega}} + \boldsymbol{\omega} \times (\mathbf{I}\boldsymbol{\omega}) = \boldsymbol{\tau}_p + \boldsymbol{\tau}_{\text{cable}} \quad (1.13)$$

These (3×3) systems can be joined together in just one (6×6) system that has the following form:

$$\begin{bmatrix} m\mathbf{E} & \mathbf{0} \\ \mathbf{0} & \mathbf{I} \end{bmatrix} \ddot{\mathbf{x}} + \begin{bmatrix} \mathbf{0} \\ \boldsymbol{\omega} \times (\mathbf{I}\boldsymbol{\omega}) \end{bmatrix} = \mathbf{w}_p + \mathbf{A}^T \mathbf{f} \quad (1.14)$$

where:

$m$ : mass of the end-effector;

$\mathbf{E}$ : identity matrix (3×3);

$\mathbf{I}$ : inertia matrix of the end-effector with respect to the end-effector center of mass reference system (3×3);

$\boldsymbol{\omega}$ : angular velocity of the end-effector (3×1);

$\ddot{\mathbf{r}}$ : linear acceleration of the end-effector (3×1);

$\dot{\boldsymbol{\omega}}$ : angular acceleration of the end-effector (3×1);

$\ddot{\mathbf{r}}$ : acceleration of the end-effector (6×1);

$\mathbf{f}_{\text{cable}}$ : Cartesian forces applied by cables (3×1);

$\boldsymbol{\tau}_{\text{cable}}$ : Cartesian torques applied by cables (3×1);

The other members that appear in the system are the one already described in the previous section. Other effects that can be taken into account to study better the dynamic behavior of the robot are all the factors involving the motors, the deformation of the cables and all the parts the system is composed by, i.e. the mechanical and electrical inertia factors that are involved in the system, friction, winch deformation, etc...

Some of these factors can not be analyzed for real-time applications but for study only, because the equations can become more complex to solve by the calculator.

Looking at the system 1.14 it is possible to understand that the dynamic of the robot is nothing but the general case of the static, where the inertia forces are also considered. In fact if one sets the acceleration  $\ddot{\mathbf{x}}$  at zero, the left member of the 1.14 would be zero and the equation would be equal to the 1.10 explained in the previous

section.

In general, in the mechanical systems there are two types of dynamic model that

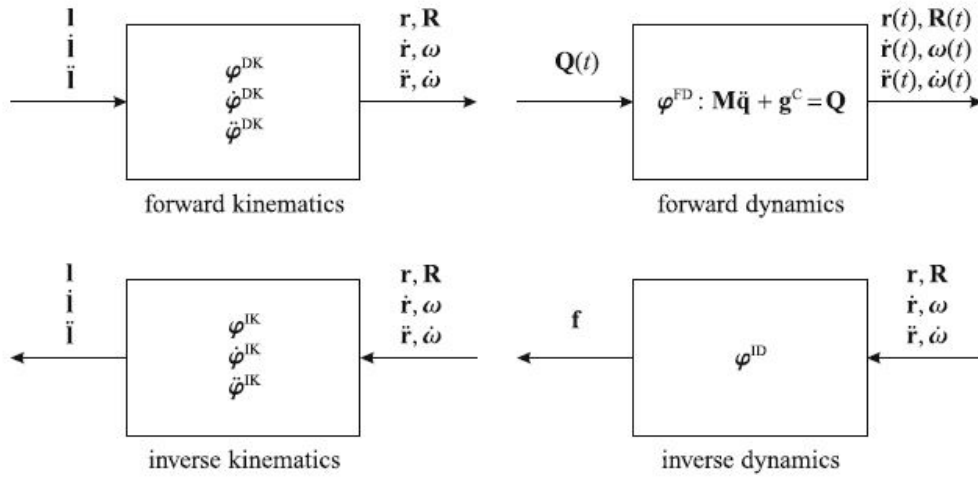


Figure 1.4: Classification of the models.

can be studied, in relation to the goal that one wants to reach. It is possible to classify them with the help of the Figure1.4:

- *Forward Dynamics*: in this case the goal is to find the parameters of motion (the pose and its derivatives) in each instant of time, knowing the external forces and torques, i.e. knowing the external wrench applied on the system; the equations to solve are coupled differential equations that usually are supposed to be put in state form in order to be solved and find the solution;
- *Inverse Dynamics*: in this case the goal is to find the external wrench of forces and torques that generates the known motion, therefore in this case the pose and its derivatives are known. This is also called *kinetostatic analysis* and the equations involved are very simple algebraic equations that can be easily solved.

The same situation occurs in the kinematics, where the joints parameters, i.e. the cables lengths, correspond to the wrench in the dynamics, while on the other side there are the Cartesian parameters, i.e. the motion parameters of the platform.

This analysis lays the basis for the robot control system, that represents the logic which the target of the task is reached with, considering all the known variables and the ones that must be computed.

There could be different types of robot control systems, depending on the goals that one wants to achieve. A typical control scheme is represented in Figure 1.5, where it is possible to notice the two different control levels: The one on the right (*Robot mechanics*) is the high-level controller, which controls and solves the maths of the physical part of the robot, the proper mechanical system. The one on the left (*Robot electronics*) is the low-level controller, which translates the information of the high-level controller and feeds them to the motors and to the electrical system, in

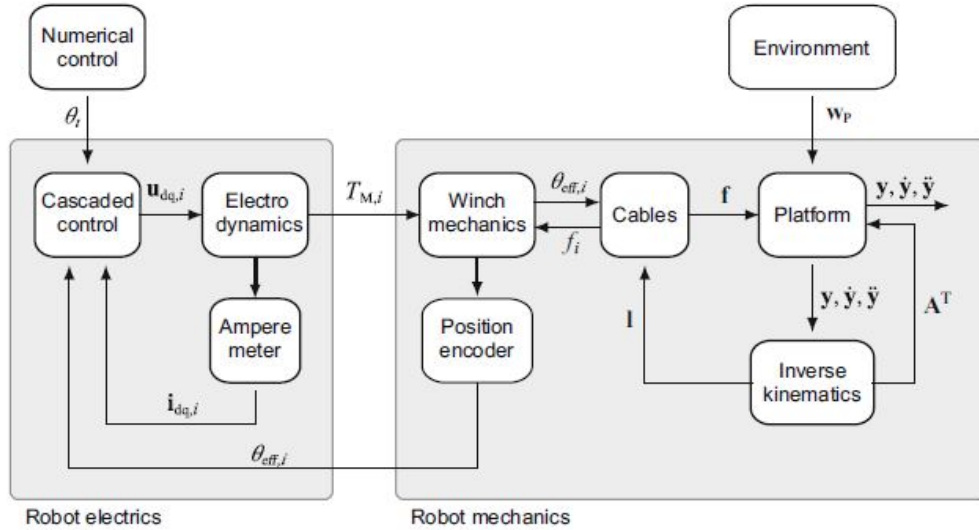


Figure 1.5: Example of CDRP control scheme.

order to achieve the targets imposed on the mechanical system.

In general, most of the studies regarding CDRPs neglect the cables mass, because otherwise the system to solve would be non-linear, and the real-time controller could possibly incur in numerical difficulties, like [9] points out. In some cases, as already said before, the mass of the cables is non-negligible, for example when the cables are very long, but since it cannot be applied in real time, it could be useful to build a simulation model that uses finite elements technique or other numerical algorithms to find a numerical solution and see the behavior of the system. At that point, it could be interesting to make some considerations about the comparison of the physical and the simulation models, underlining the differences in the behavior. An example of that case can be seen in [1] and also in [14].



# Chapter 2

## Rehabilitation with Cable Driven Parallel Robots

New technologies at doctors' disposal for surgery, like robotic arms, or new ways and materials to build tissues and prosthesis are just few examples of applications of medical robotics. In particular, this chapter wants to show the state of the art and the solutions that have been found in the field of medical rehabilitation with the help of CDPRs, a new way to conceive the rehabilitation as an active process for the patient, not just something he/she must be subjected to. CDPRs are very flexible devices that can be used in a lot of fields with different goals and configurations, thanks to the cables that allow to move high payloads at high speeds. One of the most powerful and interesting application of CDPRs is the medical and rehabilitation field, where in the last years some of the biggest innovations from a technological and therapeutic points of view have occurred. The chapter also shows, from experimental results found in the literature, that robot-aided training enhances recovery flexibility and efficiency, while reducing therapist labor. These changes can significantly improve rehabilitation outcomes for patients and moreover it can reduce social and health costs.

In most of the cases, when talking about *rehabilitation*, the discussion addresses to the recovery from an accident (e.g. spinal chord injury) and/or to develop some coordination that a subject can have lost with the progress of some diseases (e.g. ALS) or just with the age or perhaps never had (e.g. cerebral palsy).

### 2.1 Literature Overview

In the last years, technology has been to the doctors' service as an extra tool for taking the patients care and it has been worth it to develop new ways to conceive the medicine.

As far as CDPRs are concerned, the new steps in the mathematical and industrial fields have been allowing to improve their employment in medical applications, for instance rehabilitation (especially) and surgery.

A lot of wire mechanisms have been built with the aim of helping people to recover better and quicker: plenty of different geometries and configurations have been studied to reach the goal. Therefore, it could be interesting to have an overview of the state of the art of these innovative but also complex devices.

A first way to use CDPRs in rehabilitation medicine is like Body Weight Support

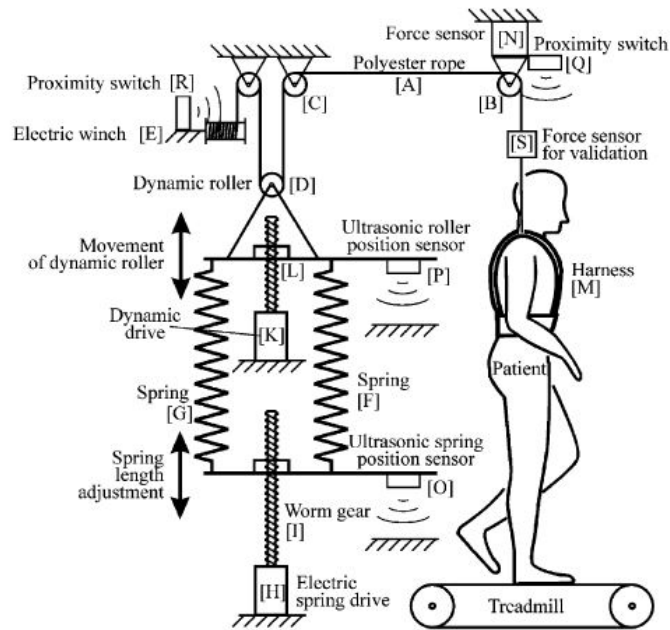


Figure 2.1: Sketch of the mechanical setup of the *Lokolift* system.

(BWS) and for this aim, there are a lot of scientific publications in literature. One of the most important is represented by *Lokolift*, the device developed in [8] which provides precise body weight unloading for patients with neurological or other impairments during treadmill training.

Body weight support systems applied to gait therapy normally consist of a harness system worn by the patient, ropes and pulleys, and a counterpoise to unload the patient. The unload capacity does represents an important characteristic for these mechanisms, which their principal aim is the one of making the subjects feel their body lighter in order to have a better performance during the gait cycle.

A novel mechatronic body weight support system for precise unloading during treadmill walking is presented in this publication. The goals that the work tries to reach are the following:

- high force accuracy with a force error clearly lower than the error of alternative BWS systems available on the market;
- full automation with static lifting capacity of up to 150 kg;
- dynamic unloading capacity of up to 80 kg.

This BWS combines the key ideas of both passive elastic and active dynamic systems. The patient is placed in a harness, which is connected to the BWS system via an 8-mm-diameter polyester rope.

The system is composed by a passive elastic spring element to take over the main unloading force and an active closed-loop controlled electric drive to generate the exact desired force. Both force generating units, the passive spring and the active electric drive, act on the patient via the mentioned polyester rope connected to the harness worn by the patient. The Figure 2.1 shows a sketch of the system. The BWS system *Lokolift* is fully automated and all its functions including lifting of the

patient and unloading adjustment can be realized with three computer controlled drives. Results of experiments conducted on humans show that the system is capable of lifting patients with a body weight of up to 150 kg out of their wheelchair and the maximum dynamic unloading is 80 kg. Therefore, it is possible to say that the aims proposed were satisfied.

After activation of the automatic unloading control, the patient gets lifted or lowered until the desired unloading force is reached, and thereafter, the system keeps the unloading force constant. The desired unloading can be adjusted at any time even during the training session without the necessity to stop the treadmill or to lift the patient. The ground force pattern recorded without BWS shows a cyclic plateau phase followed by a ground force peak before the ground force drops to its minimum. A similar ground force pattern could be observed when walking with *Lokolift*, while in contrast, this ground load pattern could not be observed when walking with other types of BWS systems.

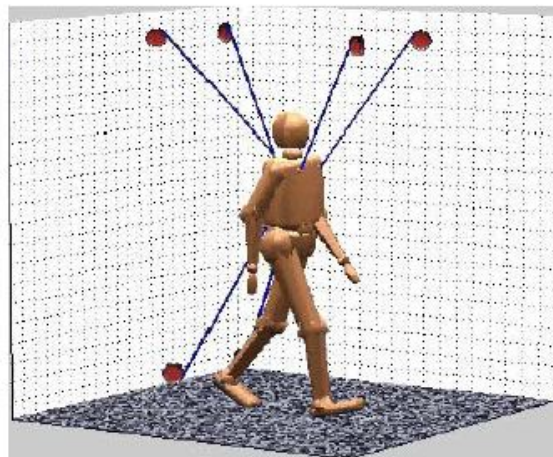
In brief, this mechanism enhances a physiological ground reaction pattern and, thus, has the potential to maximize the therapeutic outcome for human gait rehabilitation.

Another interesting cable-driven device for rehabilitation application is the one developed by Surdilovic, Zhang and Bernhardt [23] [24]. They present a novel concept of lightweight and inherently safe robotic systems for assisting the locomotion recovery therapy and training. This concept, referred to as STRING-MAN, is established on string-puppet idea and utilizes modular wire robot components and advanced artificial muscles drives: this idea addresses novel concepts towards modular lightweight and interactive gait rehabilitation devices and robots based on wire-robot technology. It opens new possibilities for assisting restoration of posture balancing and gait motoric functions.

It is pretty curious to notice that these techniques for human rehabilitation regard-



(a)



(b)

Figure 2.2: (a) STRING-MAN configuration. (b) MATMAN configuration.

ing gait were firstly tested on spinalized cats: they could be trained to walk on a treadmill with partial unweighting of their hind limbs, as stated in [2].

STRING-MAN is a powerful robotic system for supporting gait rehabilitation and

restoration of motor functions by combining the advantages of partial body-weight bearing (PWB) with a number of industrial and humanoid robots control functions. A safe, reliable and dynamically controlled weight-suspension and posture control supports the patients in autonomously performing the gait recovery training from the early rehabilitation stage onwards.

STRING-MAN rehabilitation system consists of a wire robot as shown in figure 2.2a. The wires are connected via a user interface (harness, corsage) to the human trunk and pelvis. In such a way, by closing the kinematic chains, human is uniquely integrated in the wire robots system representing “common robot platform”. This robotic structure optimally provides the requirements of controlling the posture in 6-DOFs, as well as to balancing the weight on the legs according to different gait patterns and training programs.

An innovative and attractive feature of this system is the ability to adjust the interaction control from totally passive to completely active. During the rehabilitation, the patient can be loosely harnessed with the minimum amount of wire tension required to monitor the patient’s motion. By these means, the subject is able to realistically and safely test his or her balancing capabilities. In sufficient time, the system recognizes the risk of the patient collapsing, whereupon it instigates action in order to smoothly increase tension to keep the patient upright. Finally, the system is able to bring the patient in the initial pose for further trials. This allows not only for an examination of the entire body’s ability to balance, but also trains the trunk to stabilize on fixed legs. This unique feature, analogous to how children learn to balance, was expected to be quite promising for the improvement of rehabilitation. Also, a human gait modeling toolbox was created, under the name of MATMAN, shown in figure 2.2b. It helped to support STRING-MAN development and to simulate the behavior of the system itself before the experiments on real patients were carried out.

In conclusion, the device described in these papers is a sophisticated system for gait training, providing qualitatively new functions and practicable performance for improving gait rehabilitation outcomes. Tests on real patients will help to know its concrete usefulness.

Other very interesting work is the one carried out by Gianni Castelli and Erika Ottaviano, University of Cassino, Italy, [4]. They present results on the modelling, simulation and experimental tests of a cable-based parallel manipulator to be used as an aiding or guiding system for people with motion disabilities. The principal aim is to develop a portable device to use in the daily living and in hospitals, neither too bulky nor too complex, for people who need assistance and rehabilitation: the interest was to design and implement safe and reliable motion assisting and guiding devices that are able to help end-users. The novelty of the approach is the manipulator reconfigurability in order to let the user complete different tasks just by modifying the position of end-effector attachment points and considering planar and spatial versions.

In coordination with the study of the real system, they also decided to carry out a study of a virtual model by making use of *Adams*, a dynamic multi-body software able to simulate the behavior of many mechanical systems, CDPRs included. For this aim, a validated human body model was also studied, with several simplifications compared to a real one. It was useful to include it into the system for carrying out simulation and evaluate its behavior with respect to the real one. They used

this human body model for several applications, but some modifications had to be reported based on the different implemented robot configurations. Figure 2.3 shows the model built in Adams environment and the different configurations which is feasible for. It's possible to observe that the human body can actually carry out different tasks, by moving its joints in several ways.

In this work, applications of a cable based system have been presented, as aiding and

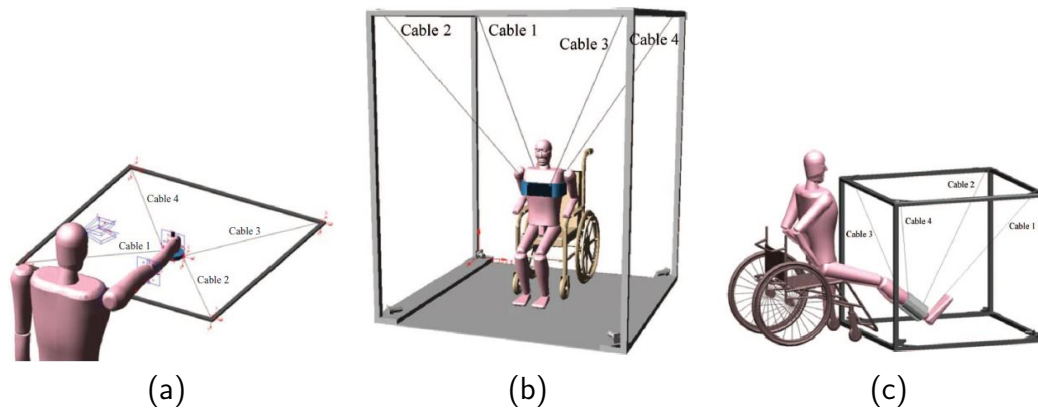


Figure 2.3: (a) A model in the ADAMS environment of the system for the motion aiding of upper limbs. (b) A model of the human body and cable-based manipulator. (c) An overall ADAMS model of the manipulator and human body for the task as an aiding motion system for the lower limb movements.

guiding motion devices. In particular, it is shown that a reconfigurable four-cable based manipulator can be used as a motion assistance device for guiding movements of the upper and lower limbs. Experimental tests have been carried out to verify the feasibility of the proposed solution: they showed that a four-cable reconfigurable parallel manipulator can be effectively used for upper and lower limb guidance by simply reconfiguring the system.

While dealing with CDPRs, one can simply think to a geometry like the ones just described, with a square frame from which the cables come out and the person stands or seats in the middle. But not always the system set-up is the same as the one just described. This is the case of the work [22], where cables are used differently from the standard cases, as figure 2.4 shows.

The paper presents a wearable upper limb exoskeleton for activities assistance of daily living with the feature of mobility. It provides 5 DOFs, for each arm, where 3 DOFs are given to the shoulder and 2 DOFs to the elbow. The cables find their applications in the joints, in order to make the exoskeleton more lightweight. Flexion/extension of the shoulder are actuated by cable-driven joint with gravity balance system and internal/external rotation actuated by belt transmission, one DOF flexion/extension at the elbow are actuated by cable-driven joint, one DOF forearm supination/pronation are actuated by double-parallelogram mechanism, and the only one passive DOF elevation/depression at the sternoclavicular joint with gravity balance system.

The fact that shows its utility for the subject and that it's feasible to apply in patients is proven by the EMG<sup>1</sup> signals that were measured during the experiments

<sup>1</sup>The electromyogram (EMG) is an electrical manifestation of the contracting muscle – this can

carried out for the aims of the paper.

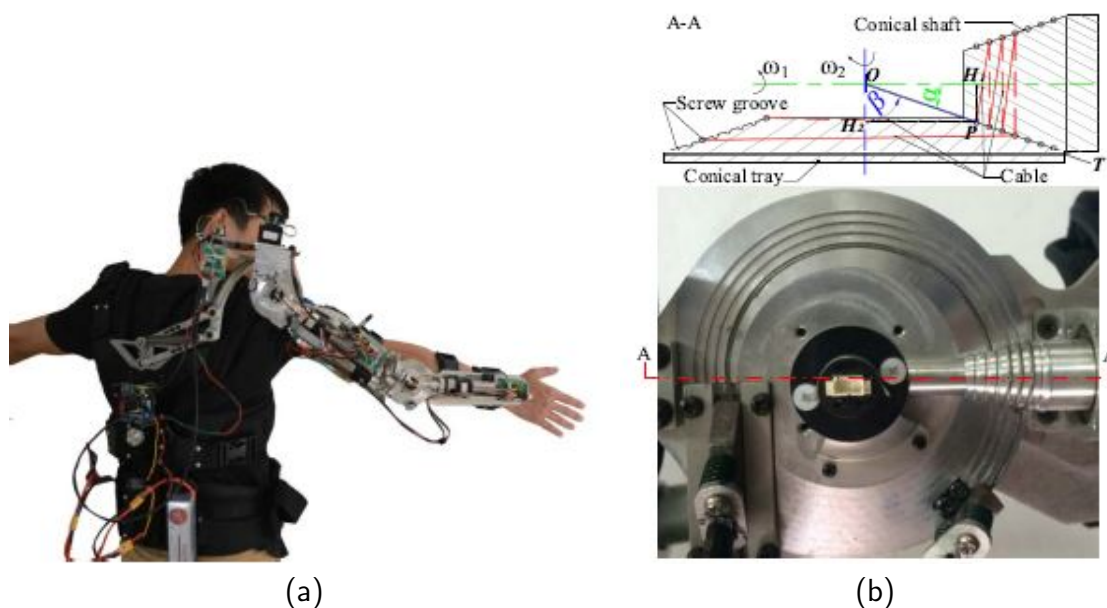


Figure 2.4: (a) Overview of the prototype worn on human body. (b) Section view of the cable-driven joint.

As seen in this couple of works, rehabilitation robotics by means of cables is a very modern topic, not just something to think as a future concept and everyday its development is advancing every day, with novelty and ideas taking advantage of cutting edge technologies.

## 2.2 The Columbia University Activity

For the topic discussed in this chapter, Columbia University has been developing a lot of new ideas and projects, working with a lot of international students coming from all around the globe. In particular, the Mechanical Engineering department is dedicated to this aim, so involved as to have established a laboratory working on this topics: the ROAR Lab (Robotics And Rehabilitation Laboratory). The RoAR Lab is focused on developing innovative robots and methods to help humans relearn, restore, or improve functional movements. The lab is housed both in Engineering and Medical campuses of Columbia University, connecting these two realities. Led by Dr. Sunil Agrawal, the lab works actively with clinical faculty from Columbia University Medical Center and hospitals around New York City. Human studies have targeted elderly subjects and patients with stroke, cerebral palsy, spinal cord injury, Parkinson's disease, ALS (Amyotrophic Lateral Sclerosis), and others. The ROAR Lab has several active projects, with different purposes and different

be either a voluntary or involuntary muscle contraction. It is a test that is used to record the electrical activity of muscles. When muscles are active, they produce an electrical current. This current is usually proportional to the level of the muscle activity. Electromyography is the study of muscle function based on the examination and analysis of the electrical signals that emanate from the muscles. More informations can be found in [6].

rehabilitative goals:

- TruSt;
- TPAD;
- C-ALEX;
- CAREX;

Let's have a quick look at these Columbia University projects regarding the topic of rehabilitation with CDPRs.

### 2.2.1 TruSt: Trunk Support Trainer

The papers [13] and [12] explain the work carried out on the Trunk Support Trainer (TruSt) as a rehabilitative cable-driven device able to improve muscular activation and enhance stability for people affected by different kinds of diseases. The figure 2.5 shows the two different configurations of the system for the two different experiments conducted on the TruSt.

The device shown in figure 2.5a consists of an active trunk belt and a passive

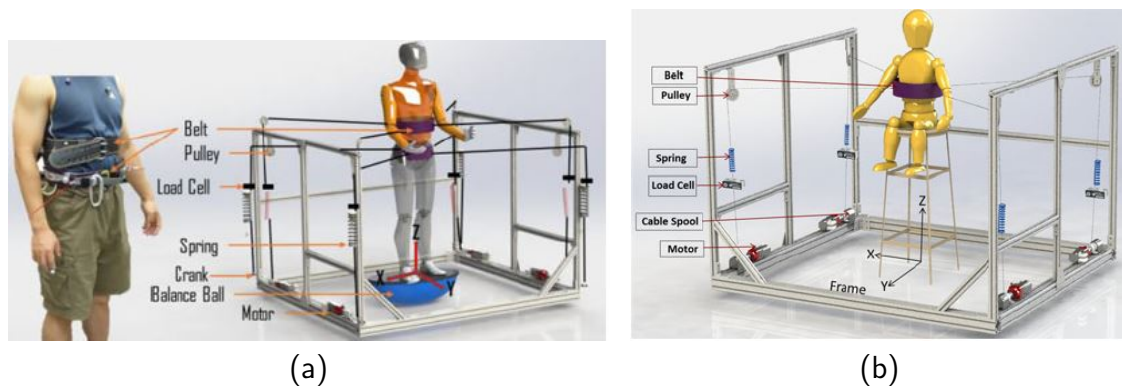


Figure 2.5: (a) Improving Pelvis Stability. (b) Enhancing Seated Stability.

pelvic belt, reinforced by thermoplastic to eliminate its deformation during actuation. Each belt is connected by four cables and routed through pulleys to a motor with encoder for active or to a spring for passive administration of forces and moments. Each cable passes through a single axis load cell powered by a 12 V DC amplifier and capable of measuring up to 890 N of force. The active trunk belt is actuated by AKM series motors and AKD drivers (Kollmorgen, Pennsylvania). A 5 cm diameter cable spool is attached to each motor shaft for cable winding. The passive pelvic belt is connected to a spring (Stiffness 2.5 N/mm) for applying resistive forces. A mechanical ratcheting crank is installed at each end to tighten and preload the spring forces as desired. All motors, springs, and pulleys are mounted on to an aluminum frame. The robotic system operates using a two-stage control, implemented using LabVIEW, PXI real time controller, and data acquisition cards (National Instrument, Austin). A motion capture system (Bonita-10 series and Vicon Vero 2.2 from Vicon, Denver) is used to record the cable attachment points on the belt and pulley for real-time force calculation.

In the second figure (2.5b) the only difference that one can underline is the presence of only one belt instead of two, because in that case the person subject of the

experiment was in a seated position and it didn't make any sense to have a belt fastened to the pelvis, while it was more useful to have one around the trunk. In fact, the belt at the trunk level helps to generate a bigger moment acting on the body, with the effect of the generation of a bigger body rotation, while by applying forces at the pelvis level the person is more subject to translational displacements, since the pelvis is located in the proximity of the body center of mass. That's the reason why, when the subject is seated, the belt at the trunk level is the one that gives the best advantages in terms of rehabilitation, because people have just to rotate their trunk to reach some points and complete given tasks and the belt in that position allow them to improve their muscle activation for that purpose. Another difference regarding the system setup from the other application discussed above, is that springs are mounted on the cables and connected to the actuators, while in the previous case they were mounted just on the passive cables. The use of springs for CDPRs can be useful when dealing with over-constrained cable robots, where the controllable DOFs are less than the actual cables connected to the end-effector. They basically allow a bigger workspace [21]. To the other side, the real-time control becomes more challenging with springs, because their presence creates a sort of delay in the system response, due to the variability of their stiffness with the elongation, that is not always constant for the whole possible spring range of motion.

These two works show how this cable-driven device can improve a person's stability after just one training session, useful either for people with disabilities and for healthy subjects, expanding their range of stability by applying a *force field* that enhances their muscular activity. Both the experiments were carried out with healthy subject in different conditions, simulating the difficulty in maintaining balance stability that actually some diseases can give.

The force field concept used in TruST and later applied in the experiments has potential benefits in the rehabilitation of posture: results have been obtained support the hypothesis that a multi-modal training promoting muscle activation, providing proprioceptive haptic feedback and allowing postural exploration without stability failure, can improve stability by decreasing the upper trunk range of motion and can couple the lower trunk and pelvis rotations. Moreover, these works demonstrate the benefits of training subjects at and beyond their point of stability failure for enhancing their maximum volitional control in seated trunk displacement with and without assist-as-needed forces.

### 2.2.2 TPAD: Tethered Pelvic Assist Device

The TPAD device developed by the ROAR Lab team is mainly shown in the paper [25]. It provides a novel approach to study the role of external pelvic forces in altering the walking effort. The main focus of this work was to apply external gait synchronized forces on the pelvis to reduce the user's effort during walking. A cable-driven robot was used to apply the external forces and an adaptive frequency oscillator scheme was developed to adapt the timing of force actuation to the gait frequency during walking. The external forces were directed in the sagittal plane to assist the trailing leg during the forward propulsion and vertical deceleration of the pelvis during the gait cycle.

The cable configuration used during the TPAD experiment is shown in figure 2.6: four cables were used to apply the desired sagittal plane forces. The hip belt was



connected to the frame top by two cables and to the frame bottom by other two cables.

The conducted experiment has been applied on healthy subjects who were sup-

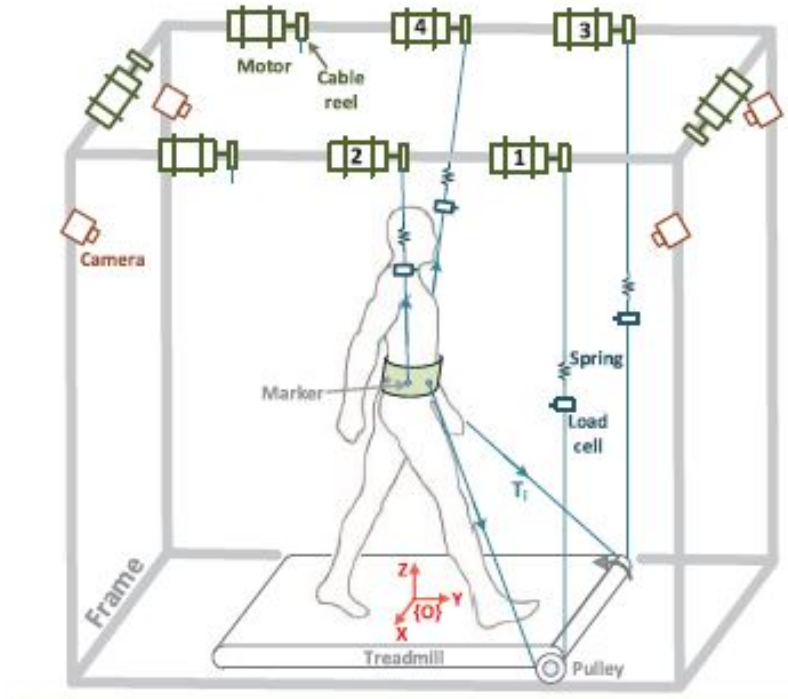


Figure 2.6: Scheme of the Tethered Pelvic Assist Device (TPAD).

posed to do two different types of training: baseline (BL), that is the first reaction to the device and to the experiment tasks, and the training session (T) that is the phase after the subject have completed several attempts of the same task. Results showed that subjects applied lower ground reaction forces in the vertical and anterior–posterior directions during the late stance phase of the gait. Moreover, the external forces applied at the pelvis could be programmed to assist a user’s trailing leg during the push-off phase of walking. Seeing these outputs, it can be also pointed out that this work can be very useful to better understand the legs joints trajectories and give some guidelines for designing prosthesis or other external assistive devices such as exoskeletons, which can be useful for patients with legs or, more in general, gait impairments, in order to reduce the overall walking effort and encourage them more to walk.

### 2.2.3 C-ALEX: Cable-driven Active Leg Exoskeleton

In literature there are plenty of solutions regarding rehabilitation robotics that use external devices such as exoskeletons that give the limbs more stiffness and coordination during motion, in order to correct dysfunctions caused by different impairments. The C-ALEX exoskeleton designed by the Columbia University ROAR Lab is one of these solutions, with the difference that it makes use of cables as actuators. Several

works have been published, but two representative papers that better describe its behavior can be [11] and [10].

The aims of these works were designing the leg exoskeleton and compare the behavior of the wearer subject while walking on the ground with the one while walking on the treadmill.

Like many rehabilitation devices developed in the past, the C-ALEX employs the “assist-as-needed” control strategy to help the ankle center move along a prescribed path. The experiment that was conducted to validate the effective benefit for the subject using the C-ALEX was carried out on healthy people, like the other devices previously described, but walking on a treadmill. The system setup will be now outlined.

As it is depicted in figure 2.7a, the exoskeleton mainly consists of three cuffs: the waist cuff, the thigh cuff and the shank cuff. The first is fixed to a height adjustable external support frame, while the second and the third are tightly connected to the wearer’s thigh and shank, respectively. To create a secure connection between the thigh and shank cuffs and the leg, a layer of medical bondage is first placed on to the subject’s leg. An orthotics with velcro liners is then strapped on top of the medical straps, while the cuffs described above are attached at the lateral side of the orthotics. The lateral distance between the cuff and the leg can be adjusted based on the person dimensions. To reduce the weight of the exoskeleton on subject’s leg, the thigh and shank cuffs are primarily made of 3D printed ABS plastic with sparse interior. The overall weight of the thigh and shank cuffs are 0.60 kg and 0.54 kg, respectively. As far as the cables application is concerned, four of them are used to actuate the exoskeleton. Every one is routed through the waist cuff: two of these are attached to the thigh cuff, and the other two are routed through the thigh cuff and attached to the shank cuff. These four cables actuate 2 DOFs of the wearer’s leg: the hip flexion/extension and the knee flexion/extension. The cable routing points are designed to be able to slide along the cuff to change the cable routing. As far as their actuation is concerned, they are driven by a servo motor with custom made cable reels, which are used to help proper winding of the cables.

Using a force-field controller, the results of the work showed that the latter was

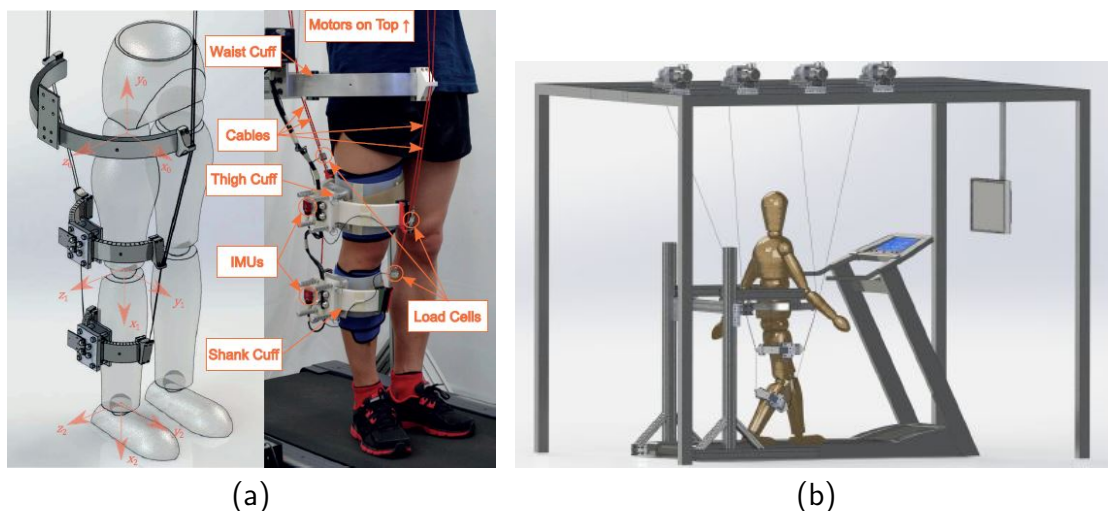


Figure 2.7: (a) Scheme of the C-ALEX geometry. (b) Using the C-Alex on a treadmill.

able to help the subject better tracking a prescribed ankle path, but there were also some limitations which were needed to be overcome. For that reason, other tests were carried out and in particular, some tests that underlined the differences between walking wearing the C-ALEX on a treadmill and on the ground, that actually should better simulate the daily behavior of its employment. The results showed that C-ALEX's controller and tension planner had no significant difference between the two use cases, therefore it has been decided to carry out experiment on the ground, in order to simulate a more real behavior of daily living. Even if subjects showed a limited adaptation over-ground with only force feedback, this showed that the architecture is capable of augmenting subjects' gait but an effective training protocol with proper feedback strategy had to be developed for overground training.

There are still plenty of new possibilities for making the system better, even though a lot of steps have already been taken, for example the inclusion of visual feedback while overground is planned, in order to better assess the assistive controller's effects over-ground and attain the desired changes in gait.

#### **2.2.4 CAREX: Cable-Driven Arm Exoskeleton**

The last project is important to underline, always carried out by the ROAR Lab of Columbia University is the one involving a cable-driven arm exoskeleton called CAREX and mainly explained in the papers [16], [17] and [5].

Actually, [16] is the first work to demonstrate via experiments with CAREX that it is possible to achieve desired forces on the hand, that means both pull and push, in any direction as required in neural training. The exoskeleton has been attached to the limb segments of a 5 degree-of-freedom anthropomorphic arm instrumented with joint sensors. These DOFs consists of three at the shoulder joint, flexion/extension at the elbow joint, and pronation/supination of the forearm.

As the figure 2.8 shows, the system consists of three cuffs: the shoulder cuff, the upper arm cuff, and the forearm cuff. Seven cables are routed through these cuffs to drive the arm: the first four cables are routed via the shoulder cuff and terminate on the upper arm cuff (these control the motion of the shoulder flexion/extension, adduction/abduction, and internal/external rotation of the arm) while the remaining three cables are routed through the shoulder cuff and the upper arm cuff and, eventually, terminate on the forearm cuff (these control elbow flexion/extension and the forearm pronation/supination of the anthropomorphic arm). In addition to the cuffs and cables, two extension bars are attached to the upper arm cuff to route the cables from the upper arm cuff to the forearm cuff. These prevent potential cable interference with the arm during motion. Since the cable attachment points play a vital role in the workspace of the exoskeleton, they are designed to be adjustable and feasible for different dimensions of different subjects. On the shoulder cuff, both radial and angular locations of cables can be adjusted, while for upper arm and forearm cuffs, only angular positions are adjustable. The shoulder cuff can be only translated along three orthogonal axes, while the upper arm and forearm cuffs can also slide along the human arm.

The cuffs of CAREX were designed to have adjustable cable routing points to optimize the "tensioned" workspace of the anthropomorphic arm. Experiments were conducted to show the performance of a CAREX force field controller when human

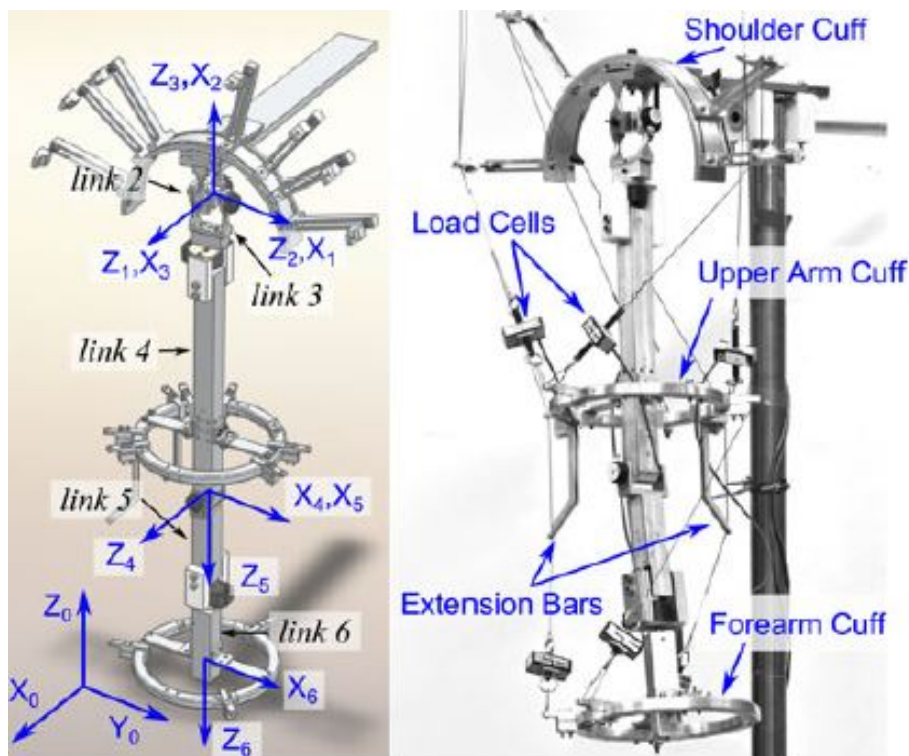


Figure 2.8: Scheme and Real Model

subjects pull the end-effector of the anthropomorphic arm to travel on prescribed paths. Statistical results showed that with proper choices of forcefield gains, the subjects were able to keep the end-effector of the anthropomorphic arm much closer to the prescribed path. Since the human–exoskeleton interface was presented to demonstrate the feasibility to transfer the exoskeleton to the human arm, other work have been carried out, actually applying the CAREX to a human arm, instead of a robotic arm, for several different purposes.

During a first study, CAREX was rigidly attached to an arm orthosis worn by human subjects, showing it can help the subjects move closer to a prescribed circular path using the force fields generated by the exoskeleton. The device was also evaluated on a stroke patient to test the feasibility of its use on patients with neural impairment, demonstrating that the patient was able to move closer to a prescribed straight line path with the “assist-as-needed” force field.

During time, the system has been developed, and a new version has been built: the CAREX-7 (figure 2.9). It includes an additional wrist module compared with CAREX, and eight cables are routed through the exoskeleton cuffs to drive the whole-arm motion, resulting more bulky but at the same time feasible for more tasks and experiments. The last show that the CAREX-7 with the new wrench-field controller can help the subjects to follow the path more closely, and this demonstrates the effectiveness of the device. This design of CAREX-7 offers significant improvements and new functionality over the previous version. The novel features are that CAREX-7 is an exoskeleton for the full human arm, including shoulder, elbow, and the wrist, with new design issues, and also controller of CAREX-7 builds on a screw-theoretic approach and assists both translation and rotation of the hand, allowing for dexterous hand reorientation, which is required in everyday tasks. It can be applied also in cooperation with EMG signal measurements too, for better

understanding the subject's behavior and improvement.

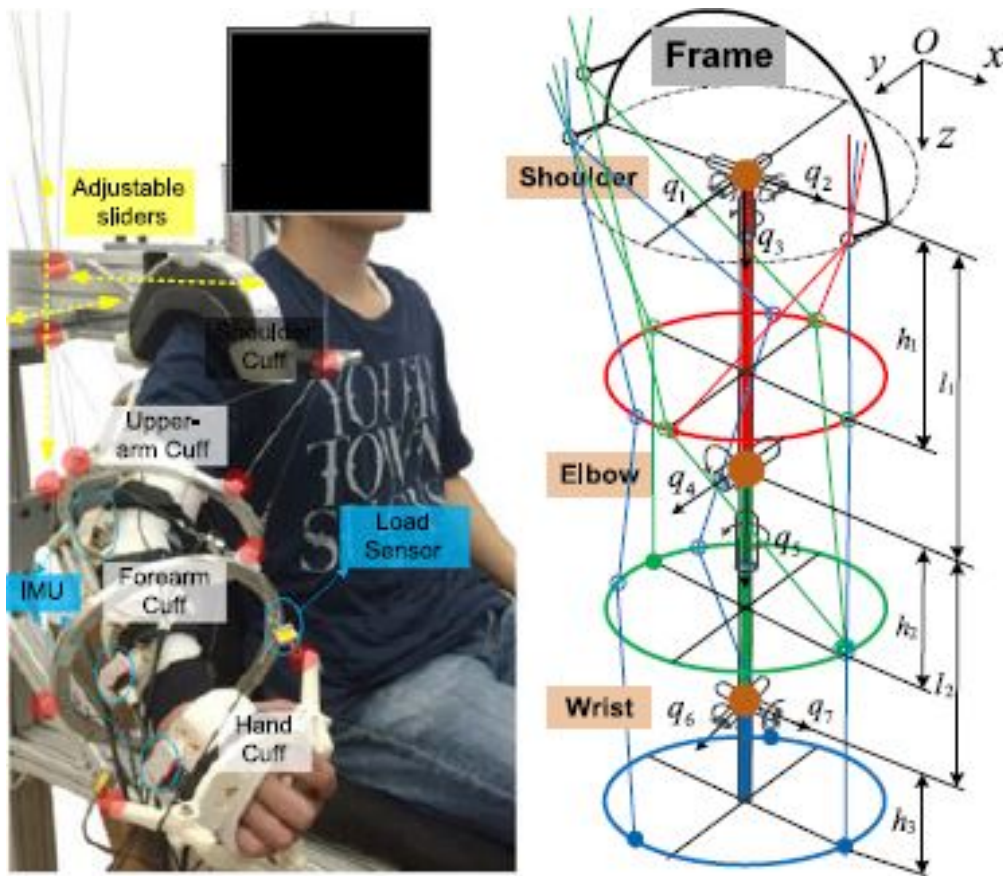


Figure 2.9: CAREX-7 overview.



# Chapter 3

## The Stand Trainer

As seen in the previous chapter, Columbia University has been working on the topic of rehabilitation cable-driven robotics very thoroughly, reaching a very important *know-how* in the field. That is the reason why new concepts and ideas are always in development, since the presented ones proved to be practically useful and not just academic scientific experiments. That is the reason why a new cable robot for rehabilitation applications is now under development. It is called *Stand Trainer* and it will be the object of this work, since it was never implemented for real experiments and data analysis before. The intentions are those of using this device to develop a rehabilitation training like the ones seen in the previous chapter: the point is to apply a certain set of wrenches in some time intervals in order to make the subject react and exert other wrenches in response to improve muscle activation for a determined area in relation with the patient's disease. This is the basic concept which the work is focused on, but the variety of applications and training ways are plenty. In this chapter, an overview of the system is proposed.

### 3.1 Description of the Robot

Figure 3.1 shows some views of the Columbia University Stand Trainer. As it's possible to notice, it consists in a cable-driven robot with 8 cables (red colored) attached to a circular-shaped belt that represents its 6-dof end-effector. By remembering the theoretical introductions to the CDPRs outlined in the first chapter, the configuration of this robot makes it a Redundantly Restrained Positioning Mechanism (RRPM). In fact, the robot is over-constrained, because it owns more cables than controllable DOFs of the end-effector ( $m = 8$  and  $n = 6$ , respectively). It's also important to point out that the anchor points on the belt are only 4, in fact as the figure depicts, two cables share the same anchor.

The robot can be described and introduced under different points of view, underlining several aspects that compose the entire mechanism and let it work properly. In the next sections they will be shown in more detail.

#### 3.1.1 The Mechanical System

Figure 3.1 also depict other uncommon elements that in conventional CDPRs have not mean to exist. The two platforms laying on the ground are implemented because

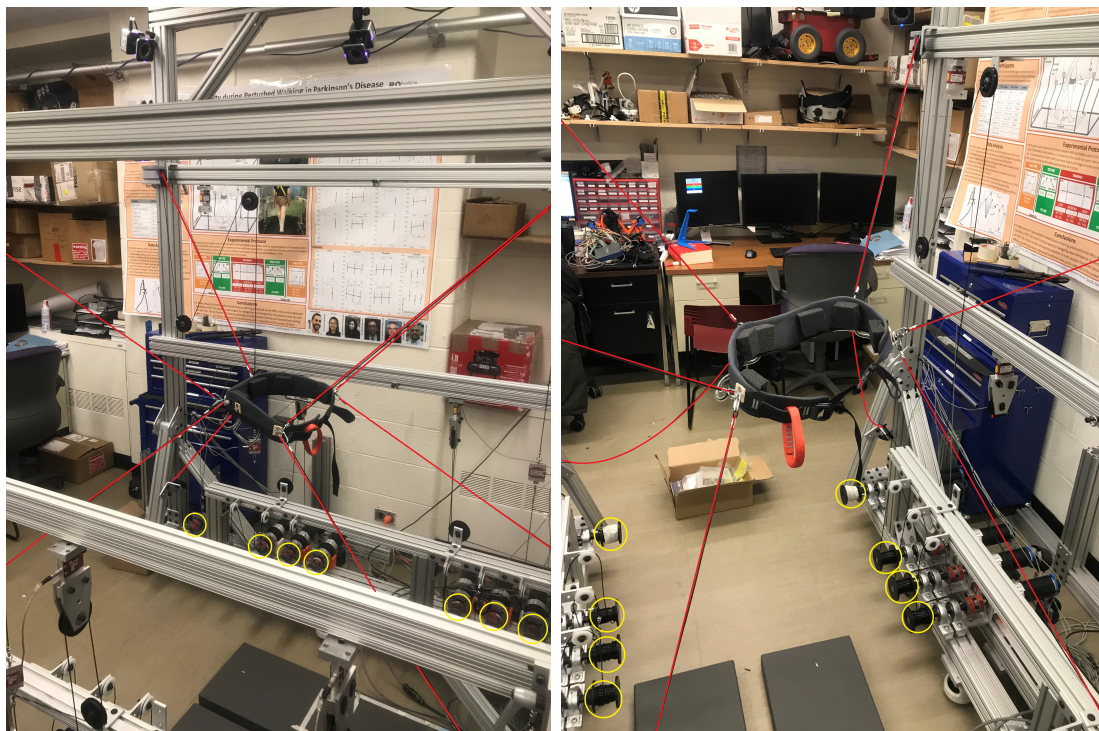


Figure 3.1: Views of the Stand Trainer by ROAR Lab - Columbia University.

the robot employment has to do with people, therefore its setup must be different to the more common industrial robots. These are two platforms (one for each foot) that can measure the applied force on their surface. They are useful to know the ground reactions of the subject standing on them while wearing the belt and working. By the use of the system in real time applications, in every instance the position of the center of pressure (COP) of the subject body may be known thanks to these two platforms, and it can be also useful for detecting whether a person is taking a step or not: this can be inferred by wondering if the applied force is pushing the subject beyond his/her limits of stability. Therefore, it can be useful in order to know either the distribution of the person weight, whether its posture is correct or not and where is the resultant reaction force positioned.

Always on the bottom part of the device, it's possible to notice that 7 motors (yellow circled in figure 3.1) for each side are fixed on the frame, for a total of 14 motors, which correspond to 14 cables. In the configuration shown in figure 3.1, only 8 are actually used, 4 for each side. The other 6 are not yet employed but present for future development thus. The fact that the system has 14 actuators makes it very flexible for several applications, in fact, as already said, it's possible to change its setup (the number of cables) and obtain a different type of cable robot able to satisfy different requests and tasks, being feasible for several subjects with various kinds of impairments.

In the first chapter, it's been pointed out that in order to solve the statics of a cable-driven robot it is necessary to solve the kinematics too, because the wrench generated on the end-effector is correlated with the cable tensions by means of the Jacobian matrix. The last one varies with the geometry, meaning that this matrix characterizes the system: when a geometric parameter changes, the Jacobian matrix changes too. After having observed this concept again, it's important to underline



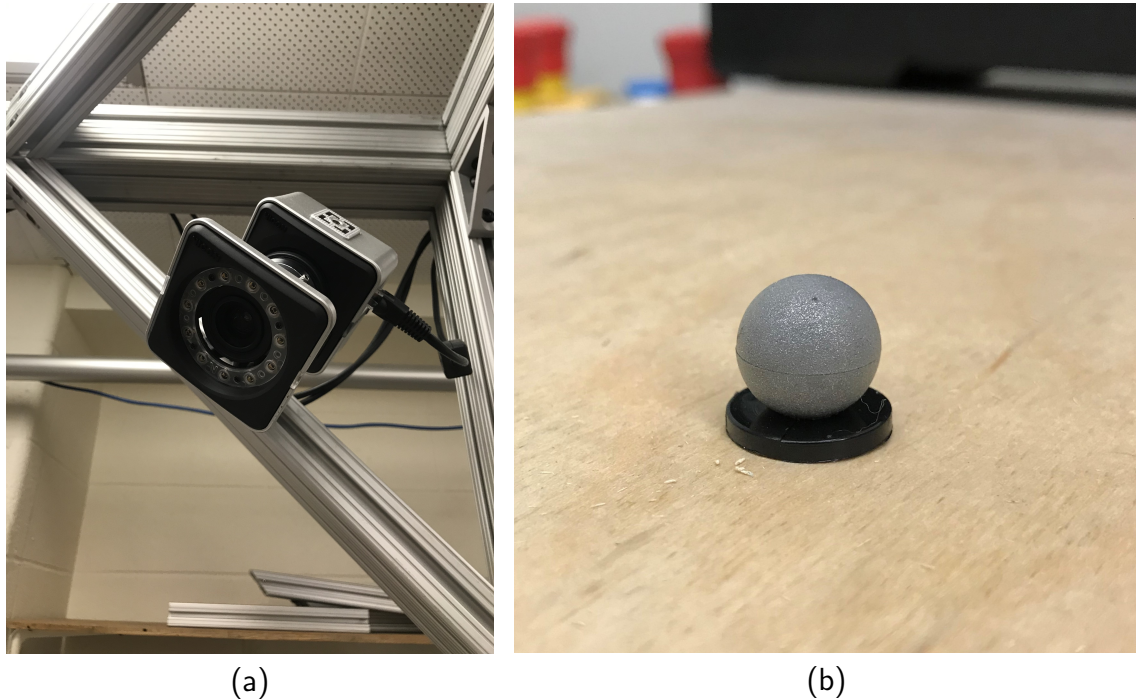


Figure 3.2: (a) Vicon Camera. (b) Example of a Marker.

a fundamental element of the system that makes the resolution of the real-time algorithms and the data analysis much easier and convenient: the *Vicon* motion capture system.

It consists in a series of 9 cameras like the one shown in figure 3.2a that catch the position of the system elements in real-time with a sample frequency of 200 Hz. It is worthwhile to underline that the cameras don't observe the entire environment, but they only identify some points that reflect light thanks to their external surface. Apparently, these points look like simply gray markers with a sticky bottom part, but in reality they are high reflective markers that cameras can easily detect in the infrared spectrum. They are supposed to be put on the sites of more interest for the motion evaluation, depending on the application. One of them is shown in figure 3.2b. These markers reflect the light and send it to the cameras that act detecting their positions. At least two cameras must see a marker in order to let it be recognized by the system. This setup can be very expensive, but at the same time it can be very powerful, because of the great amount of opportunities that it gives, such as detecting the COM position of the subject during its motion, positions of the legs and the arms, cable lengths and other interesting measures for data analysis. Also it allows to keep the rest of the system mechanically more simple, with less sensors that would be essential without the Vicon system. In the final stage of post-processing, the data that has been collected during the tests is analyzed in a software called *Nexus*, provided with the Vicon system, where data analysis can be done and many results can be post-processed.

The last important mechanical part to discuss are the sensors measuring the cable tensions during the machine operations. With the two platforms described before, they are the only force sensors present in the device and they measure the force that the cable is exerting when the robot is operating. Figure 3.3 shows its appearance: it

is nothing but a load cell (LSB302 Futek, California) that can work both in traction and in compression, with a 1335 N (300 lb) as maximum load capacity. The way the cable tension is measured has been one of the topic of this work, therefore it will be discussed more in detail later on.



Figure 3.3: Cable Tension Sensor.

As far as cables are concerned, they are 2.5 mm diameter composed by steel with a black rubber shell all around, that allows to protect the cable itself and let them have more adherence to the pulley grooves. Moreover, the rubber shell allows not to hurt patients when they are using the robot, which is something that could happen in case the cables were made of steel (because sometimes it might happen that the subject hits against them with the arms during training).

They are routed on pulleys in a complex way, because all the motors are positioned on the ground and some of them are too close one to the other to let the robot have enough operational workspace. Therefore, it is needed to let them pass through several pulleys before reaching the belt out.

As far as the routing is concerned, cables are coiled onto the motor drums without any winch or screw able to guide them, but they are simply rolled in an undefined way, as figure 3.4 shows. That means the radius the cable is routed around changes with the amount of cable there is on the drum. This also means that the rate of change of the cable length is never known exactly, which translates in not knowing its length for each time instance. This issue is overcome thanks to a control algorithm, which exploits the Vicon camera system in order to know, at every time instant, the position of the belt and the components of the unit cable vectors. Therefore the winches on the motor drums are not needed and the geometry can be kept more simple: the cable length rate of change is known thanks to Vicon.

In order to keep the cable on the drum and avoid to let it slip around, the adopted solution is shown in figure 3.5: basically, a little hole on the frontal surface of the black plastic drum in the figure has been drilled, and the cable slipping around the drum is avoided by using an oval sleeve, remaining fixed onto the surface.



Figure 3.4: Undefined cable routing around the motor drum.

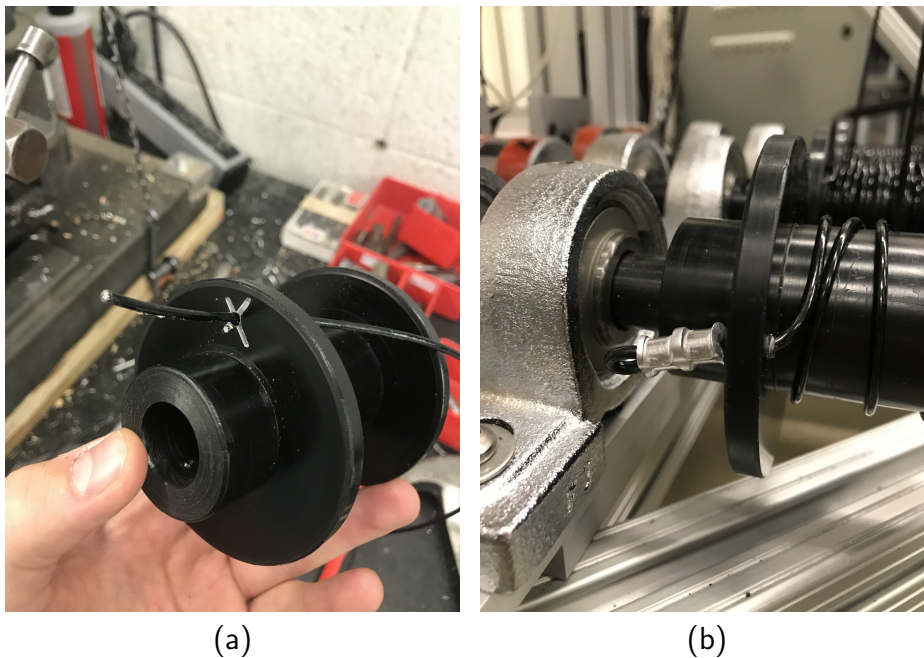


Figure 3.5: (a) Detail showing the hole on the frontal surface of the drum. (b) Detail showing the oval sleeve compressed that block the cable passage and avoid the slipping.

### 3.1.2 The Control System

After having discussed about the mechanical parts which the robot is composed by, a basic control system description will be outlined, in order to figure out its logic. First, it's important to understand that a robot can always be controlled in several ways, such as position control or force control.

The first uses a position as the target, which can be the one of the motors or the one of the end-effector and the control system tries to reach that position with a certain effort.

In the other case, the target can be either a wrench applied to the belt or a torque applied to the motors, depending on the aim of the robot. Together with the applied wrench, the controller needs to know the time interval that the wrench has to insist for.

Usually, in rehabilitation robotics the control is delivered always on the force, because in the opposite case, there wouldn't be a direct control of the applied wrench onto the subject of the experiment/therapy, in fact there could be some peaks of forces (due to the will of reaching a certain position) that can hurt the patient and cause him/her some serious injuries.

By going more inside to the control system, it can be divided into two different parts: the High-Level Controller and the Low-Level Controller.

#### - *High-Level Controller*

This side is the one that controls the mechanics of the robot, the more concrete part.

Basically, the user imposes a certain wrench that must be applied on the end-effector, as said at the beginning of the chapter, in order to make the person resist to that wrench. The geometry of the system is known from the Vicon real-time data that allows to know the cable vectors and the positions of the belt markers that at the same time allow to compute the Jacobian matrix of the system.

$$\mathbf{A}^T = \begin{bmatrix} \mathbf{u}_1 & \cdots & \mathbf{u}_m \\ \mathbf{b}_1 \times \mathbf{u}_1 & \cdots & \mathbf{b}_m \times \mathbf{u}_m \end{bmatrix} \quad (3.1)$$

This matrix is the one that, multiplied by the vector of cable tensions, gives the wrench set imposed by the cable system (equation 1.11). Since the vector of cable tensions is unknown, in order compute it, it is necessary to provide an optimization method (the system is not squared). In this case, the problem is solved imposing the continuity of the cable tension, i.e. minimizing the distance between two consecutive tension values. This goal is reached using a quadratic solver that adds the following equation to the system:

$$\min \frac{1}{2}(\mathbf{t} - \mathbf{t}_p)^T(\mathbf{t} - \mathbf{t}_p) \quad (3.2)$$

being  $\mathbf{t}_p$  the cable tension vector at the previous time instance and  $\mathbf{t}$  the cable tension vector to compute at the current instant.

At this point, by knowing the tensions that the sensors have to read, the Low-Level Controller is the one that regulates the cable forces.

- *Low-Level Controller*

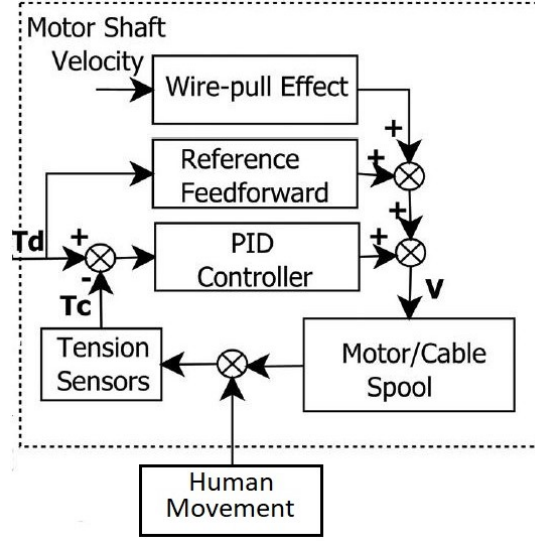


Figure 3.6: Logic scheme regarding the low level controller

The low-level controller runs at 1 kHz using LabVIEW PXI real time controller. Figure 3.6 gives an overview of the low level control logic. To achieve the desired cable tension  $T_d$ , previously computed by the high-level controller, a specific current is provided to the motors. This is relative to a voltage calculated using a pre-measured motor constant  $K_M$  relating voltage and cable tension. To provide that voltage, the desired cable tension is first compared with the one computed by sensors  $T_c$ , giving a closed loop PID based feedback term  $T_{FB}$  that represents nothing but the error between the two measures. This one is then multiplied by the motor constant and it returns a first term representing the voltage provided to the motors that is able to put the error at zero. In parallel, there is an open loop feed forward system that uses the value of  $T_d$ , now identified as  $T_{FF}$ , that returns the second amount of voltage supposed to be added at the first one, in order to finally obtain the entire amount. Basically, the voltage provided to the motors yields

$$V = K_M(T_{FF} + T_{FB}) \quad (3.3)$$

For this cable-driven systems, to keep tension in the cable  $(T_{FF} + T_{FB}) > 0$ , the lower bound of the feedback term is set as  $T_{FB,low} = -T_{FF}$ . However, if the subject pulls the cable away from the motor, extra negative input is required to compensate motor friction and unspool the cable reel. Only for this pulling case, the controller decreases the lower bound of the feedback term respect to the speed of the cable reel.

## 3.2 Cable Tension Measurement

In every CDPR, even though the control system deals with the statics and kinematics of the robot by solving the maths, it is always good to have some feedbacks regarding

the effective cable tensions while the system is working. This is needed for safety reasons first (for the device and for the patient) and second to better understand if the robot is working good or if there can be some issues in the control system that generate a dysfunction.

That is the reason why the Stand Trainer adopts the sensor shown previously in figure 3.3. The sensor is a load cell that measures the axial force caused by its deformation under the cable load. As pointed out before, this type of sensor works both in traction and in compression, but clearly for cable robots the only interest is the first way.

In the old version, the robot had all the sensors (one for each cable) mounted like the figure 3.3 shows: basically, the cable was cut, the load cell placed in the middle and cables extremities attached to it.

In this way, it is logic that the force measured by the load cell placed the same one that the cable was applying on the belt, neglecting the friction on the pulleys, therefore for the PXI controller it was straightforward to transform the measure reading to the cable tensions. In that way the motors were trying to reach the target cable tension imposed by solving the statics and the kinematics of the robot. On the other side, the disadvantages of this way to mount the sensors were several: first, if the person moved too much for some reasons during the use, the sensor could hit the frame of the robot, with dreadful consequences for the hardware; second, even though they don't weigh too much, sensors generate inertia forces while moving, which introduce some errors on the read tension and generate at the same time annoying cables vibrations: they affect the measure introducing a lot of noise and disturbance.

Those are the reasons why it was time to think to another way to mount the sensors, in order to have much less noise in the measure and don't damage them anymore. This new way has taken inspiration from the paper [19], where a new system for tension monitoring in cable-based parallel architectures is described.

### 3.2.1 A New Way of Cable Tension Monitoring

As previously said, the tension monitoring with the load cells mounted along the cables generates a lot of noise in the measure, increase the probability of damaging the sensors and moreover some vibrations on cables are excited due to the sensors inertia. All these consequences are due to the sensors' motion during the use of the robot.

To solve these problems regarding the cable tension measurement, another idea was taken in consideration: by keeping the same sensors, it was better to fix them on the frame to avoid their movement, which is the cause of all the issues explained above. The figure 3.7 describes very well the idea.

The main concept which this solution is based on is that the cable pulls with a force  $F$ , the pulley the cable is routed on is attached to the sensor which at the same time is fixed to the frame. This solution provides a much better quality of the tension monitoring, giving less noise to the measure and moreover it preserves the integrity of the sensor, without the risk of damaging. On the other side, there is the issue of the force value read by the load cell. In fact, theoretically, by having two perfectly straight and parallel cables, the value that the load cell can read should be exactly the double of the cable tension, because it measures nothing but the reaction force

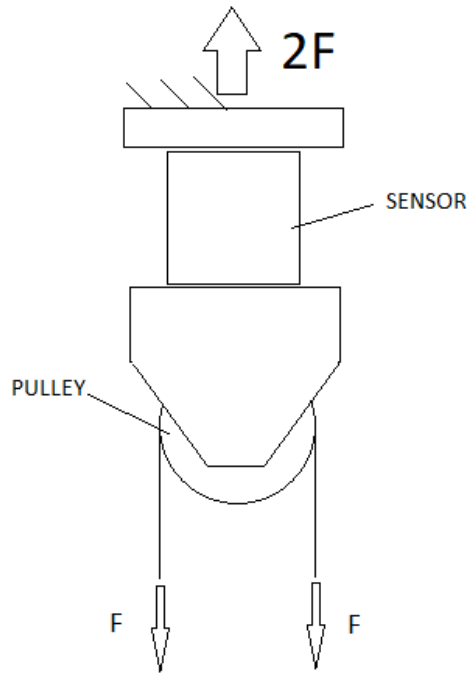


Figure 3.7: Sketch of the new tension monitoring system.

that keeps the system fixed to the frame.

It wasn't easy to find right away a practical way to mount the system, but some time has been needed in order to think how to realize this useful solution. Basically, the idea that has been developed was to fix the sensor to the frame by using a screw that could connect an aluminum flange to the highest part of the sensor, and then connecting the flange with the sensor mounted on onto the frame using other screws. After that, the pulley had to be fixed between two plates (one for each side of the pulley), which were fixed at the same time to an aluminum block by using two screws. Every component, apart from the sensor, was conveniently designed and machined for the aim. With the help of the software *Creo Parametric* it has been possible to design the parts needed to realize the idea. After that, the drawings has been sent to the machine shop of the Columbia University Mechanical Engineering department and the parts manufactured.

In the following figures is possible to have an idea of the realized components and the whole system.

Figure 3.8 shows the three elements designed and machined, able to compose the new system. In figure 3.9 it's possible to see the CAD assembly and its realization. In this way, the main disadvantages found mounting the sensors along the cables have been overcome. In fact, now that the sensor is fixed, its integrity is guaranteed and the noise caused by the cable movement and vibration is deleted.

By the way, this solution is not exempt from defects or issues. In fact, the theoretical model explained in figure 3.7 is valid under the hypothesis that the cables are ideally parallel, lying on the same plane and therefore that system is perfectly symmetric. Only under these assumptions, the force read by the sensors is exactly the double of the cable tension. In practice this is not possible, because there will always be some errors in terms of non-symmetry or non-parallelism between the cables.

For these reasons, there had to be a way to verify if the system worked well as

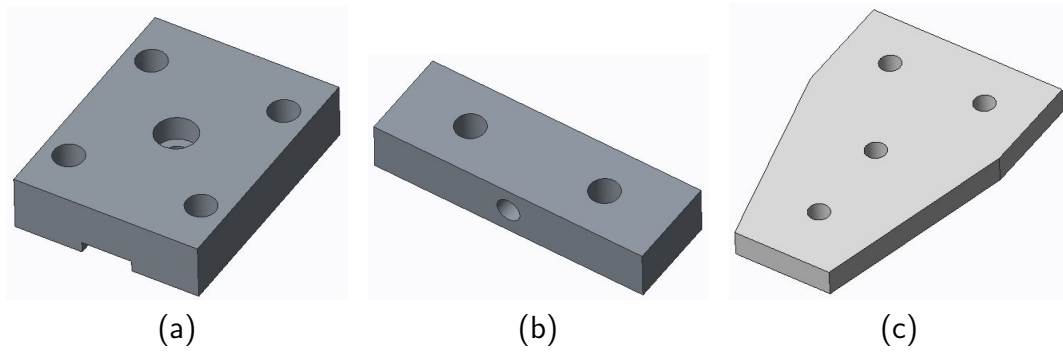


Figure 3.8: (a) Aluminum flange. (b) Aluminum block. (c) Aluminum plate.

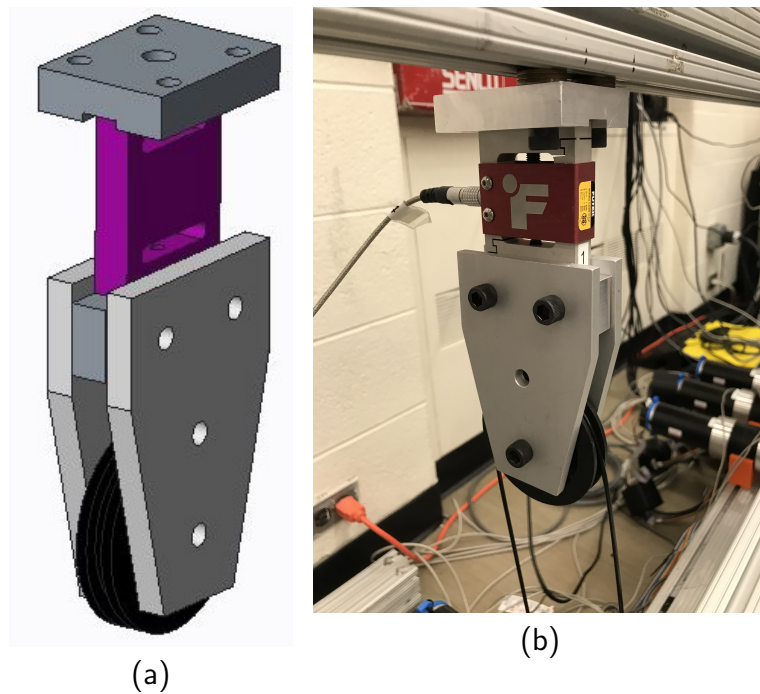


Figure 3.9: (a) Creo assembly. (b) Assembly realization.



expected or not. The solution to this issue was to mount a sensor along a cable as it was done before, and at the same time to mount the new solution for the same cable. At this point, another hypothesis had to come up: the tension *statically* measured from the sensor attached in between the cable is the correct one, i.e. the real force that the cable applies is the one measured by the sensor mounted along the cable. This hypothesis can be real in static conditions, when the cable is not moving. This is because otherwise, if it was in motion, there would be the same issues explained before for the sensor along the cable, having the wrong behavior.

Thus, it was needed to statically characterize the system, that means it was needed to correlate the two measures of tension monitoring and introduce this correlation in the LabVIEW code that controls the robot, in order to measure the correct cable tension even when the sensor along the cable wouldn't be mounted on anymore.

### 3.2.1.1 Tests for the Correlation

Since in practice cables are not parallel like the ones in figure 3.7, the system is not theoretically perfect and it was needed to correlate the two measures by carrying out some tests.

For each bottom-part motor (the motor where the routed cable ends on an anchor of the belt coming from the lower level) the new cable tension monitoring system (*sensor2*) was mounted, and at the same time, another sensor (*sensor1*) was also mounted along the cable. In this way, the control system implemented on LabVIEW was able to detect two different measures: *sensor1* and *sensor2*. A lower bound on the cable tension was chosen, from which the test started, and it was taken by the value measured by the *sensor1* on the cable. The captured data started to be recorded at a sample frequency of 200 Hz.

After the data was recorded, its analysis has been carried out on Excel and Matlab. In particular, this analysis consisted in several steps. First, the data acquired by *sensor2* in terms of tension had to be correlated with the one acquired by *sensor1*: a correlation line was built and its slope and the *y*-intercept were computed using the *Least-Square* analysis. Calling with:

$s2 = x$ ;

$s1 = y$ ;

and  $N$ : number of points recorded;

these equations hold:

$$a = \frac{\sum_{i=1}^N (x_i - \bar{x})(y_i - \bar{y})}{\sum_{i=1}^N (x_i - \bar{x})^2} \quad (3.4)$$

$$b = \bar{y} - a\bar{x} \quad (3.5)$$

where

$\bar{x}$ : average value of  $x$  data;

$\bar{y}$ : average value of  $y$  data;

$x_i$ :  $i$ -th  $x$  data value;

$y_i$ :  $i$ -th  $y$  data value.

The equation that comes out after this analysis will be:

$$y = ax + b \quad (3.6)$$

with

$a$ : slope of the correlation line between  $x$  and  $y$ ;

$b$ :  $y$ -intercept of the correlation line between  $x$  and  $y$ ;

Also it can be useful to evaluate if the correlation between the two entities is good.

This work is done by the linear correlation index  $R$  that has the following form:

$$R = \frac{\sum_{i=1}^N (x_i - \bar{x})(y_i - \bar{y})}{\sqrt{\sum_{i=1}^N (x_i - \bar{x})^2} \sqrt{\sum_{i=1}^N (y_i - \bar{y})^2}} \quad (3.7)$$

The more it is close to 1 or  $-1$ , the better the correlation between the two entities  $x$  and  $y$  is.

The plots regarding the measures before the correction are shown in the figure 3.11. On the  $x$ -axis the values of the *sensor2* are indicated, while on the  $y$ -axis the values of the *sensor1*, that represent the cable tensions. As the figures depict, the values

	<b>MOTOR_1</b>	<b>MOTOR_2</b>	<b>MOTOR_3</b>	<b>MOTOR_4</b>
<b>a</b>	0.5204	0.49988	0.52673	0.49942
<b>b</b>	-0.10818	0.4147	-0.58113	-0.11851
<b>R</b>	0.99973	0.99967	0.99969	0.99992

Figure 3.10: Parameters of the correlation computed with the *Least Square* method.

of the  $x$  and  $y$  axis seem to be more or less one the double of the other, with some errors that justifies the correction with the *Least Square* method, without trivially divide by 2 the *sensor2* values.

The coefficients computed with the method explained above are shown in figure 3.10.

From these coefficients, one can notice that the value of  $R$  remains very close to 1, that means there exists a very good correlation between the two values of the measured tension.

It is pretty interesting to notice that the values of the slope are very close to 0.5 that represents the perfect theoretical condition. That means new way of cable tension monitoring is working properly and the system is mounted correctly, without too much parallelism errors regarding the cables setup.

Moreover, it can be interesting to analyze the error with respect to the right value, even though in general the system is working pretty good for most of the motors. Basically, the absolute value of the error  $e_i$  has been computed as the difference between the *sensor1* value and the correspondent of *sensor2* divided by 2, as the theoretical case is supposed to be.

$$e_i = \left| y_i - \frac{x_i}{2} \right| \quad (3.8)$$

Since the value of  $e$  increases with the increase of tension, the percentage of the error just computed has been evaluated with the equation 3.9, with respect to the tension value recorded by the *sensor1*:

$$\%e_i = \frac{e_i}{y_i} \times 100 \quad (3.9)$$

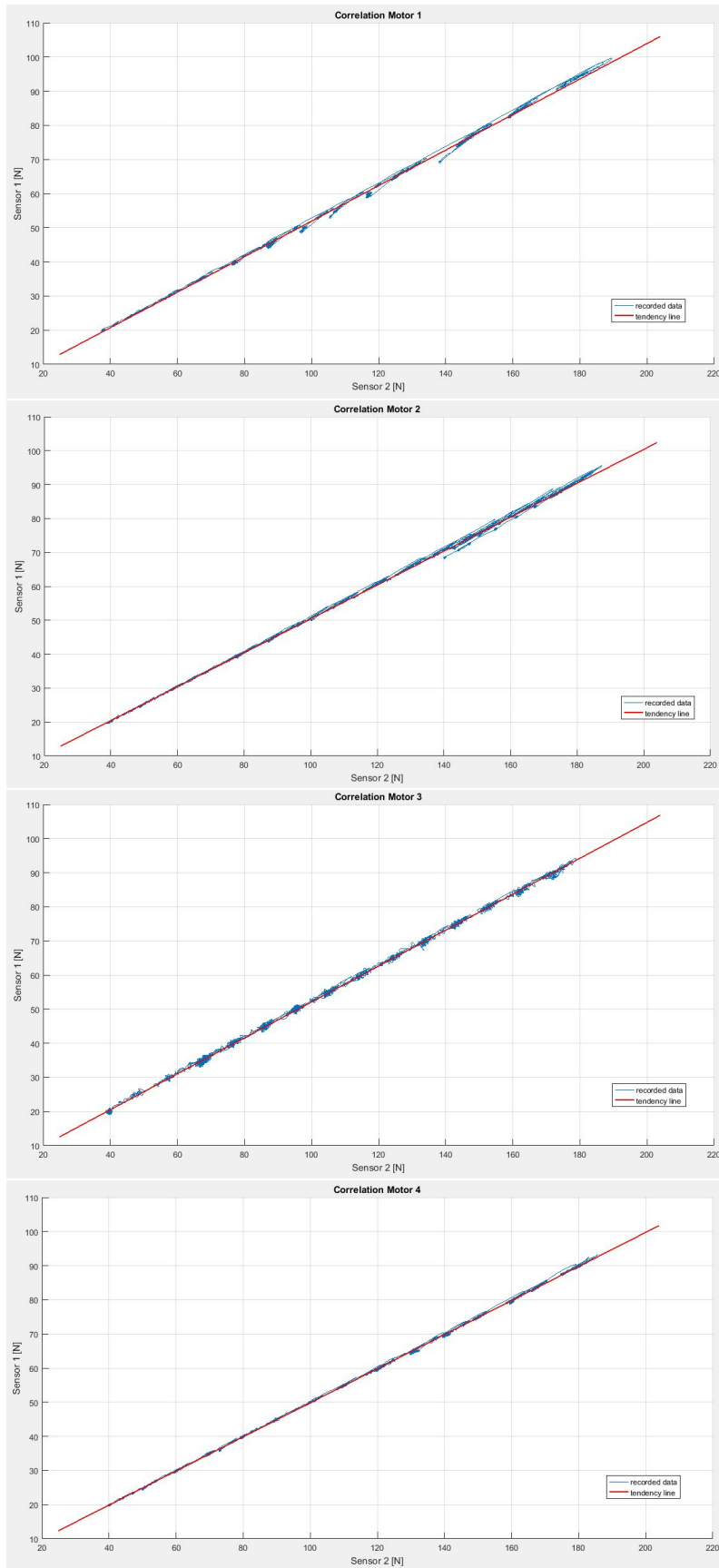


Figure 3.11: Plots of the 4 motors on which the test has been carried out.

The plots showing the errors can be seen in figures 3.13 and 3.14.

The yellow and the green lines represent the mean values of the errors, absolute and percentage respectively, for each motor during the entire test.

Now that the correlation model has been built, it is time to apply the correction factors to the LabVIEW code and see what are the errors occurring in this case. It's important to underline that each tension value is different from the one relative to another motor, because the robot is not symmetric, therefore there are also significant differences in the locations of each sensor with respect to the frame. Because of this, the need of using four different correlation models does make sense and it's worthwhile. In fact, this is proven by the coefficients written above: even though they are very similar, they result different one from each other, that means this choice makes sense.

Applying the correction to the model, the plots coming out from the data analysis on Matlab are shown in figure 3.15. At first glance, one can notice that even though the tensions measured and corrected seem good, a hysteresis phenomenon occurs, because the data recorded in these tests (after the correction) started from a lower-bound tension value, rose until an upper bound, and then went down again, while in the other case described before, the test carried out provided for just the first raising part, where the tension increased from the lower-bound to the upper-bound. These two values (upper-bound and lower-bound) were established previously from the experience of the data collected from other experiments carried out before the beginning of this work. That's the reason why in this case the hysteresis born. This can be due to the deformation of the cable, that even though it is small, it does occur and its effect is translated in this behavior.

	<b>MOTOR_1</b>	<b>MOTOR_2</b>	<b>MOTOR_3</b>	<b>MOTOR_4</b>
<b>a</b>	1.01209	1.01666	0.97976	1.02128
<b>b</b>	-0.70105	-1.13529	0.89204	-0.41972
<b>R</b>	0.9986	0.99949	0.99726	0.99905

Figure 3.12: Parameters computed after the correlation with the *Least Square* method.

Applying another time the *Least Square* method, it's possible to compute another time the coefficients shown in the equation 3.6. This time the correlation must be 1:1 between the values of *sensor1* and *sensor2*, so *a* is expected to be close to 1 and *b* close to zero, as it was before. Figure 3.12 shows that the values are the ones expected and it can be pointed out that the model works efficiently.

Another phenomenon which can cause this behavior of hysteresis is the friction between cables and pulleys: for the tests just described it is not so important since they were conducted in static conditions, but in the dynamic behavior, it does exist and has more important effects which can cause a variation of tension on the final part of the cable, the one that exerts the force on the belt, with respect to the part where the tension is measured.

If one wanted to delineate everything, since with the new cable tension monitoring system the effort the load cell has to resist is the double of the cable tension, another

issue this model introduces is that the maximum cable tension the sensor could read before being damaged will be the half of the previous case, where the cable was mounted along the cable. This occurs because when the load cell measures its limit force (300 lb) the cable tension will be approximately the half (150 lb). Practically, for the aims of the device, it is not an issue, because it never happens to reach such a high cable tension (667 N).

This description has been carried out to introduce this new cable-driven robot built by Columbia University and have an overview of it. This was done also by discussing the new way of cable tension monitoring introduced in this model, which allows a more efficient way of working, preserving sensor's life and avoiding noise in the tension measure.

Now, it can be interesting to build a simulation model of the Stand Trainer, capable to simulate the behavior of the entire system and compute the wrench that the subject wearing the belt is applying in order to increase muscle activation and reach the aims of rehabilitation. This can be useful in order to build a training session program for people with physical diseases to improve their motion coordination and find an easier way for their daily living.

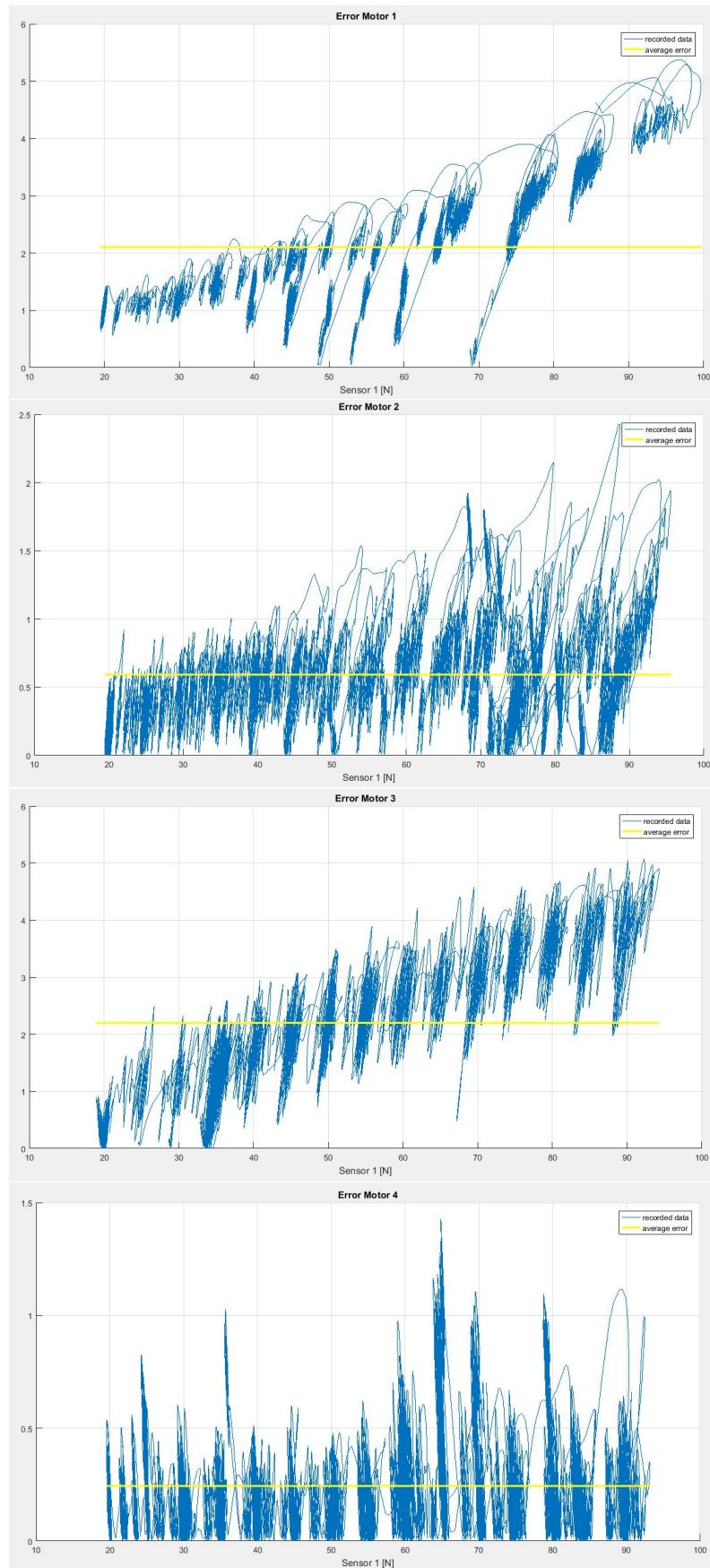


Figure 3.13: Absolute value of the error obtained without correction.

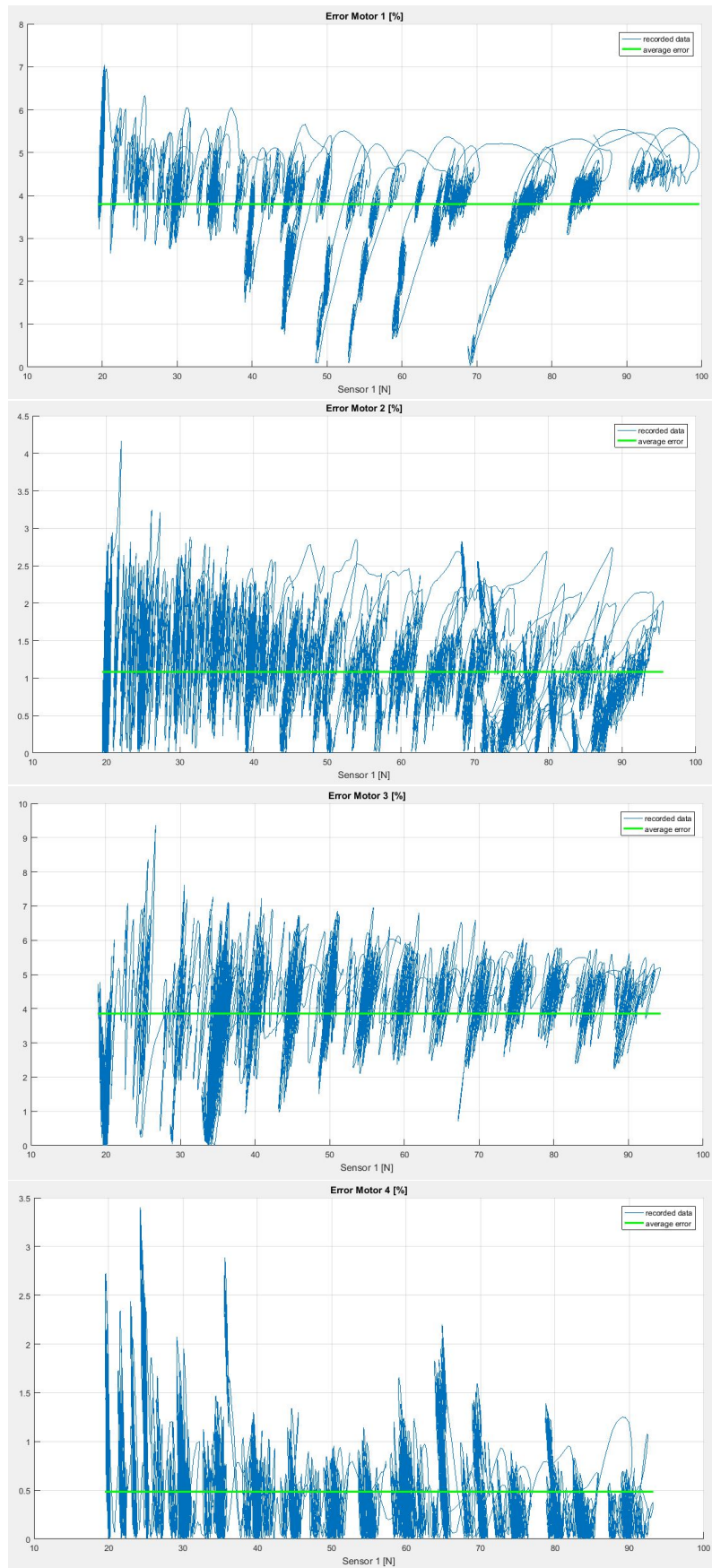


Figure 3.14: Percentage of absolute value of the error obtained without correction with respect to the *sensor1* values.

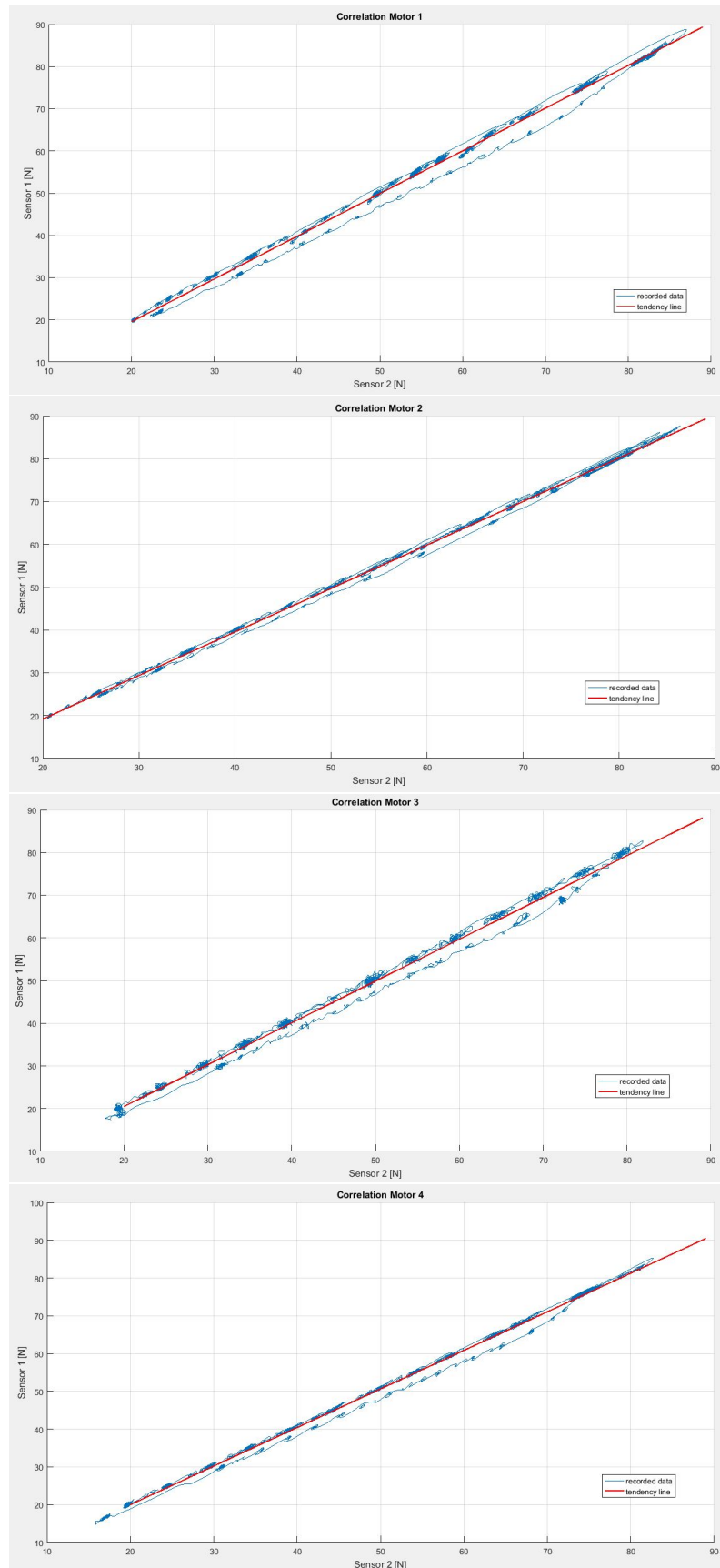


Figure 3.15: Plots of the 4 motors on which the test has been carried out after the correction with the coefficients computed after the correlation model was applied.



# Chapter 4

## Adams Simulations

Nowadays more than ever, mechanical systems have reached a very high level of complexity and non-standard phenomena may be time-consuming to investigate in practice. For example, it could be useful to see how the system responds to a certain force, or to a certain law of motion, or maybe what is the correlation between two entities that one wants to measure while it is working. Or more, it could be interesting to assess the validity of the control system analyzing its behavior after some modifications.

For sure, the topic becomes very delicate when working with people, or in other words, when they are the subjects who the system is acting on. Great care is needed not to hurt them, but at the same time effectiveness is needed as well in order to obtain the desired results. This can be even amplified when the subjects are disabled people, who can't apply too much resistance, being more subject to the system's actions, having more probability to get injured.

For these reasons, a simulation software can be used to study the problem: it can be capable to simulate the system behavior, and when working with people replay the system's effects on them, which means replaying their reactions while it is applying forces.

The main advantages to have a simulation model of the system are the possibilities to check if a certain change can be worth it and what are the global effects while applying it, without changing the real system, but applying the change on the virtual one. If the model has a behavior that can be considered similar to the real one for some reasons, with a certain approximation order, that modification will give a correct evaluation of the new mechanism's behavior and will help the decision making process. In the majority of the cases, this aspect is translated also in money and time saving, therefore it could be worth it working with this approach.

Here, as anticipated in the previous chapter, a simulation model of the Columbia University Stand Trainer is developed, in *Adams View* by MSC Software, a multi-body software on which the dynamic behavior of mechanical systems, among other things, can be described and their analysis carried out.

### 4.1 Introduction to the software

A quick introduction to the software is needed in order to familiarize with its way of working. Adams is one of the most widely used multibody dynamics and motion analysis software in the world. Adams helps to study the dynamics of moving parts,

how loads and forces are distributed throughout mechanical systems, and to improve and optimize the performance of products.

Adams multibody dynamics software enables to easily create and test virtual prototypes of mechanical systems in a fraction of the time and cost required for physical build and test. Unlike most CAD embedded tools, Adams incorporates real physics by simultaneously solving equations for kinematics, statics, quasi-statics, and dynamics. Utilizing multibody dynamics solution technology, Adams also runs nonlinear dynamics in a tiny fraction of the time required by FEA solutions. Loads and forces computed by Adams simulations improve the accuracy of FEA by providing better assessment of how they vary throughout a full range of motion and operating environments.

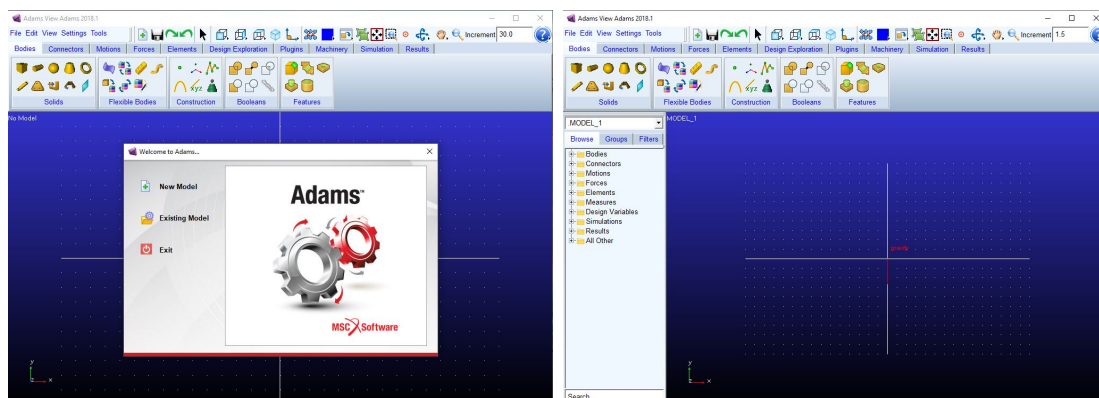


Figure 4.1: Software Overview.

When modeling the system it is vital to be able to easily process the data obtained. Thus, one of the most important and useful resources that Adams offers are the *Measures*, which in some cases can be very convenient to use for analyzing results, saving a lot of time while post-processing the data. For instance, the coordinates system of the virtual model and the one used to record the data from the real system can be different, and this was the case of the Stand Trainer. For that reason, it is possible to change the position and orientation of the reference system in order to have an equivalent data set and compare it with the real one. After that, it is possible to create a *Measure* and see the displacements, velocities, forces, etc... as if the global reference was that new one.

A lot of other interesting and very useful things are provided by Adams. For the aim of this thesis, it has been needed to introduce some non-standard elements that can be found on the *Machinery* part of the software: the *Cable Systems*. In Adams, cable systems can be modeled using mainly two methods: the *Simplified Method* and the *Discretized Method*.

### 4.1.1 Simplified Method

The cable's mass and inertia are neglected, dummy parts with pure kinematic constraints are used to track the tangent lines between pulleys, angles between dummy parts of same pulley determine cable length that's around each pulley, differential equations are used to track cable span physical length from integrating the pulleys'

angular velocities, cable span tension forces are computed from the difference between the cable span's pure geometry and physical length, appropriate action-only forces are applied on the pulleys to replicate the effect of cable contact with friction. Talking about the application, the simplified cable provides a very fast solution which generates accurate loads on the pulleys as long as cable mass and inertia effects are negligible with respect to transmission effect. Winching effects are accounted for in terms of the addition and removal of cable length from the system. Pulleys can be offset from base plane and rotated in and out of plane during design time and disengage from the cable during the course of a simulation. Finally, the limitations that can be found are that all pulleys must be initially engaged with the cable (as mentioned above they can disengage during the simulation), they must have a circular shape and must not move so much during the simulation that the wrap order (routing) changes. Winching effect of increased pulley diameter is not accounted for.

For two consecutive pulleys, one of the pulley plane shouldn't intersect through the center of other pulley.

### 4.1.2 Discretized Method

Using this method, the cable is discretized with appropriate parts, joints and forces (mass, inertia, beam-formulation-based longitudinal, bending and torsional stiffnesses) and contact with pulleys is applied with forces using an optimized analytical formulation (sphere/ cylinder) in the plane together with an appropriate lateral guidance approximation. The cable segments are represented graphically as spheres so as to exactly reflect the geometry used in the cable-to-pulley contact detection process. Even though cylindrical graphics may be more intuitive, they could potentially be visually misleading.

Talking about the application, the discretized cable will compute precise cable vibrations and forces on pulleys in scenarios where the mass and inertia effects of the cable are important. Also, pulleys can be offset from base plane and rotated in and out of plane during design time and disengage from the cable during the course of a simulation. This method is also useful as a reference for result comparison with equivalent simplified cable analyses.

Finally, all pulleys must be initially engaged with the cable (as mentioned above they can disengage during the simulation) and must have a circular shape. Moreover, all winching effects are neglected.

For two consecutive pulleys, one of the pulley planes shouldn't intersect through the center of other pulley.

For the simulation of the Stand Trainer, the *Simplified Method* was chosen, because, as a first approach, it was necessary to create the simplest model that could better replicate the system before pretending to have a very accurate but very complex model that considered a lot of different factors. For future works, it can be interesting to change the type of method used to solve the system, modelling the cables with the discretized method and adding some other real factors. This method introduces less simplifications, making the system more consistent with respect to reality.

Other information about the software and its way of work can be found in [18].

## 4.2 The Stand Trainer Models

As seen in the previous chapter, the Stand Trainer consists in a CDPR with 8 cables attached on a belt composed by four anchor points, meaning that every cable shares its anchor point with another one (more precisely, with the one of the same side, but opposite height level). The person is supposed to wear this belt and be subject to a certain cable wrench which has the aim to improve several muscles which can be weaker or less developed for some diseases.

The aim of this part (that is also the aim of this thesis) is to build an Adams model that could recreate the same behavior of the real system described in the chapter 3, but most importantly a model able to compute the wrench that the subject under training exerts during the tests. Several simplifications are introduced:

- the end-effector of the robot is just a belt modeled as a torus with the same internal diameter of a male's average pelvis diameter, thought as a perfect circumference (25 cm);
- the belt is a rigid body while the cables have the possibility to be deformed;
- the belt has the same mass of the healthy subject on which some test were carried on (90 kg);
- the belt has the same inertia matrix of an average male subject ([15], [7]) computed with respect the body COM reference frame, neglecting the non-diagonal values. A consequence is that the virtual human who is wearing the belt is acting as a dead body, therefore the system is subject to all its inertia, because it doesn't apply any external wrench on the belt to resist the motion;
- since the previous simplification holds, the body can't take any step during the tests, and its feet are considered fixed to the ground;
- the robot is symmetric with respect to the sagittal plane, while in reality there are some differences regarding the locations of the pulleys;
- the cables are thought as massless, therefore the effect of the gravity and their inertia during the motion are neglected;
- the disengagement of the cable from the pulleys is avoided, that means the cables can't come out from the constraint imposed by the pulleys;
- the cable's material is set as steel with a Young's Modulus equals to 200 GPa, but in reality it has also a rubber shell on the external that can change its value.

After all these simplifications have been introduced, it's important to understand how to actuate the model, that means, to decide which quantities are supposed to be imposed in order to better replay the real behavior. As it has been pointed out in the previous chapter, the Stand Trainer is controlled in force, meaning that the Cartesian wrench is the input of the control system and then it translates this wrench applied on the body COM in a vector of cable tensions by solving the geometry of the mechanism. This is usually done while working with people, because it is safer for them. Serious injuries, in fact, can occur by using a position control. At the end

of the logic path regarding the force control, the low-level controller translates cable tensions information in a voltage supposed to be applied to the motors, as it was shown in figure 3.6.

A previous test had been run, where the user was applying some Cartesian wrenches to the subject who was wearing the belt. In the meantime, it was possible to collect data about the cables tensions, motors angular velocities, and position of the body center of mass (COM) with respect to the inertial frame. By the knowledge of the real data, it has been possible to make a comparison between them and the data obtained from Adams simulations.

Three different virtual models has been created:

1. The motors velocities are applied to the model;
2. The cables tensions are applied to the model;
3. The motion of the end-effector and the cable tensions are applied to the model.

The next section will discuss the models just introduced and their simulation outputs, proving the two main thesis that force control leads to a smoother subject treatment during the rehabilitation training and that the combination of the belt motion with the cable tensions on the virtual model provides high accuracy compared with the real system. That will be the reason why with that model it will be possible to find the wrench that the subject exerts during the training session.

### 4.2.1 Model 1: application of the motors velocities

The first Stand Trainer model that has been developed is the one shown in figure 4.2, where the cables are attached to the ground from one side, and to the belt to the other. In order to let the system work properly, the motors velocities recorded from the real tests have been assigned. The main hypothesis under which this model has been built is that its behavior should be good in terms of system kinematics, because, since the motors' laws of motion are imposed and the geometry of the system is similar (similar Jacobian), the motion of the end-effector should be well-replayed. However, a probable drawback could be lied in the cable tension values, introducing a too much high-valued wrench applied on the subject compared to the real one.

Moreover, this model is the one that results more faithful to the system from a geometrical point of view, because the anchor points from the motors sides are attached to the ground and the lengths of the cables follow a specific law of motion that is the one followed by the cable routed around the motor drum. This hypothesis was done even though it can not be totally exact, because, as pointed out in the chapter 3, the motors have got no winches and the cables are routed in an undefined way around them. In the next subsections, it will be possible to notice that the other two models are not built like this one.

As pointed out in the previous section, it is possible to notice that the system is perfectly symmetric with respect to the sagittal plane, while the real model is not, having small misalignments, which for the aim of this work have been neglected. Another interesting things to notice are the rigid links where the anchor points are connected.

As stated above, in this model a law of motion to the motors was assigned, but as

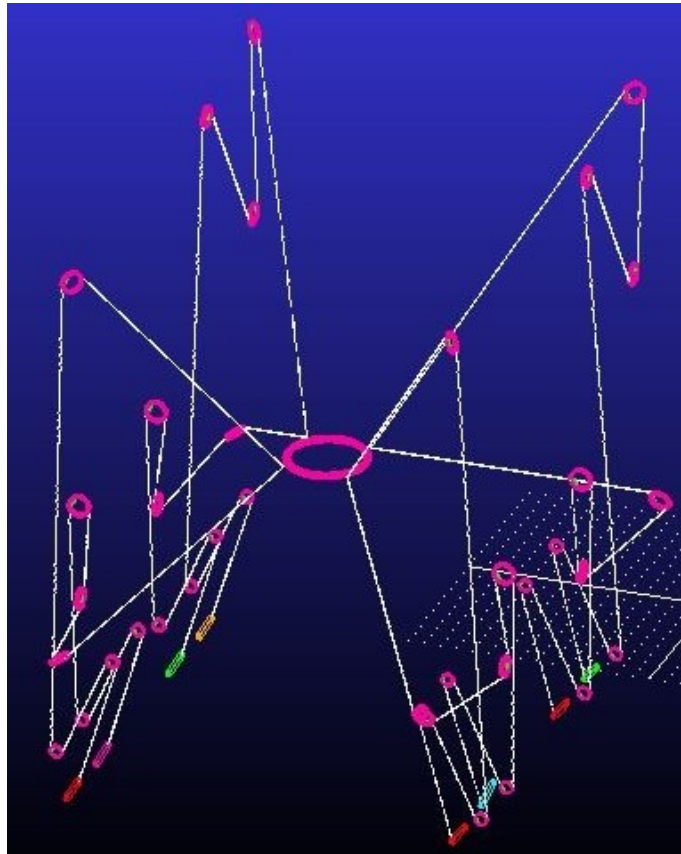


Figure 4.2: Stand Trainer Model: "Model 1".

it is possible to see in figure 4.3, there isn't a proper model of the motor, but the system has a rigid link that shares the anchor point with the cable. This link lies along an axis parallel to the Global Reference Frame  $x$  axis and there is one of them for each cable, for a total of 8 links. The reason why they have been put there is because in order to change the cable length and have the consequent motion of the end-effector, it was necessary to create a state variable in the system that joined the rotation of that link with the length of the cable it was attached to.

Basically, it's been necessary to create a rotational joint in correspondence with the

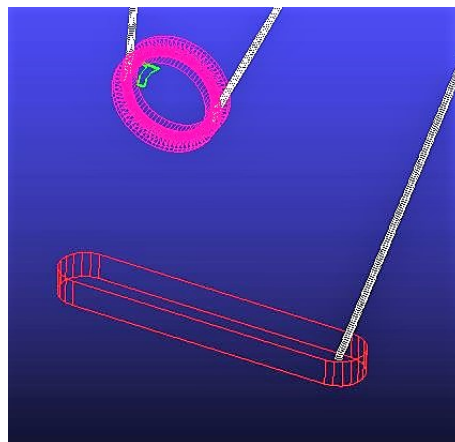


Figure 4.3: Example of anchor point attached to the link.

anchor point where the link was attached to, having the rotational axis laid along

the Global  $x$  direction, as if in that position there was the motor. After that, a law of motion of the joint was created, based on the numeric data collected from the real model that gave the motors velocities. It was applied to the joints using a cubic spline to connect the sampled recorded points one to the other. This law of motion was connected to the length of the cable by a state variable that controlled the cable winch: basically, while the link was rotating, the cable length was changing with the same amount of the link rotation, with an amplification factor represented by the radius of the drum (20 mm). This amount coming out from the last product was nothing but the amount of cable that was being coiled on/off the drum, while this was rotating with that law of motion.

Now that the model is set, it is possible to run a simulation and see what happens to the behavior of the system. The simulation run-time was 18.49 (the amount of recorded time during the tests on the real model) seconds and the splines were sampled at 200 Hz, that means one point every 5 milliseconds, for a total of 3699 points. The time-step size of integration during the simulation was set at the same step-size of the spline, that is 5 milliseconds.

#### 4.2.1.1 Model 1 Outputs

The outputs which the work is interested in are the comparisons between the real data recorded previously and the virtual data obtained from these simulations, in terms of Cartesian wrench applied on the end-effector, cables tensions, position of the belt COM. The latter was not computed with respect to the Adams Global Reference Frame, but it has been necessary to create another Reference Frame in the same position as the one of the real test was set, relatively to the belt COM. In figure 4.4 it is possible to see that reference frame within the yellow circle. This coordinate system setup has been used for the other models too, allowing a very good comparison with the real data, since it is in the same position as the one used for the real model tests.

The simulation results for the *Model 1* show a strange behavior of the system compared with the real one. In fact, the position of the belt COM follows the one recorded during the real test with a certain degree of approximation that can be acceptable considering all the simplification explained at the beginning of the section and that the Jacobian of the virtual model is different from the real one. In figure 4.5 are shown the plots representing the movements of the belt during the two tests (real and simulation), giving a direct comparison between them.

Cable tensions are those that look more different compared to the real data. By looking at the plots, they assume extremely high values, with an order of magnitude of thousands of Newtons, while the real ones stays under two hundred. In figures 4.6 and 4.7 it can be noticed that either cable tensions and forces applied on the belt are extremely high and not feasible for this type of application like rehabilitation. Otherwise, the subject would be hurt in a very serious way, putting his/her life in danger.

As one can understand from the figures, these data contains a lot of numerical errors that will be discussed after having presented all the models and the tests, during the post-processing steps. Now, it can be worth it to underline the fact that this type of control doesn't get along with the fact that the end-effector is actually a human subject, needing a much smoother actuation.

Finally, it's possible to point out that the initial thesis about this model is

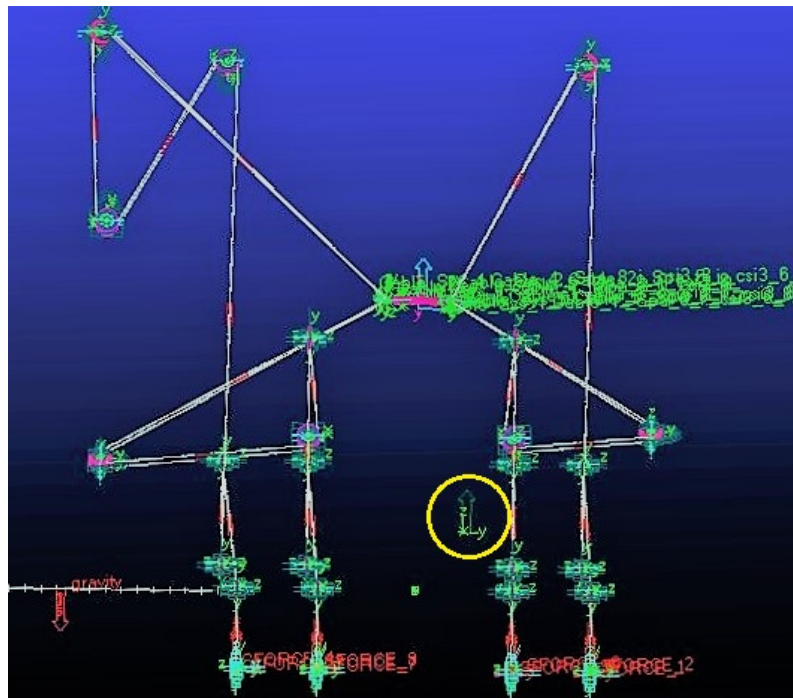


Figure 4.4: Reference Frame with respect the displacements are referred to.

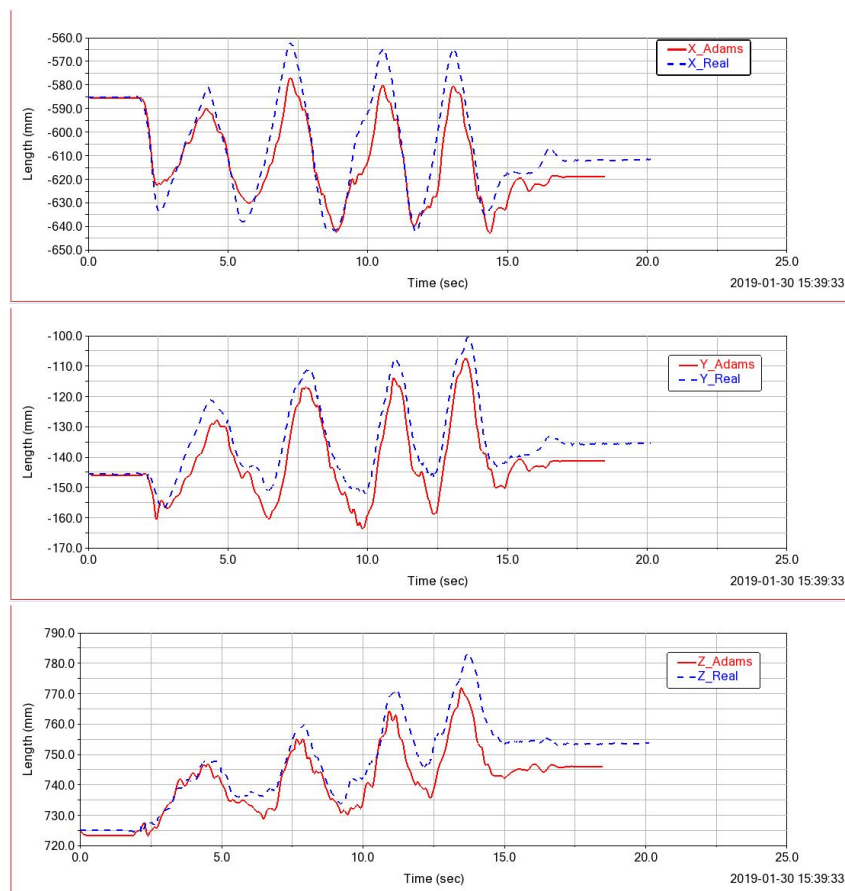


Figure 4.5: Belt Cartesian Position Comparison - Model 1.



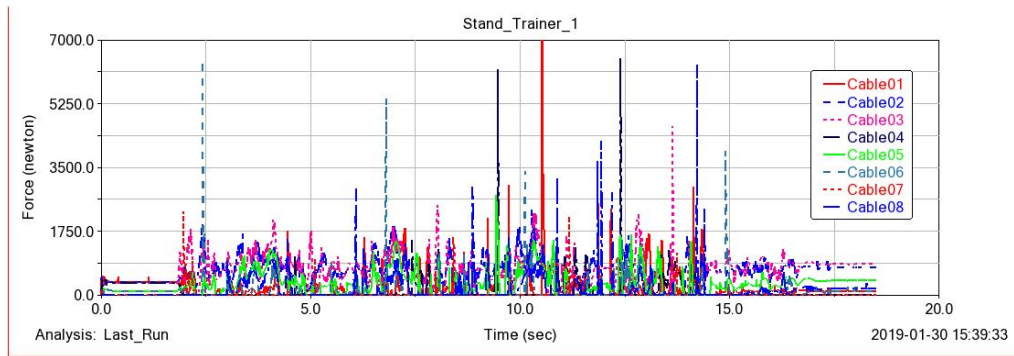


Figure 4.6: Cables Tensions - Model 1.

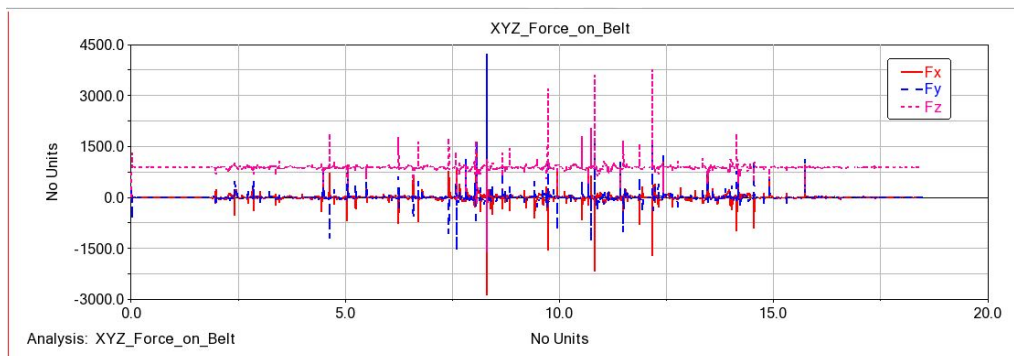


Figure 4.7: Forces on the belt COM - Model 1.

confirmed: its behavior is good in terms of system kinematics, because the motion is well-replayed as the plots in figure 4.5 show, but it is not correct from the forces point of view, since the wrench applied on the subject is too high and can cause serious injuries if applied for real.

### 4.2.2 Model 2: application of the cable tensions

The second model that has been built to try replaying the behavior of the Stand Trainer is the one that uses cables tensions as inputs. This time, the effective wrench applied by cables to the end-effector is the one that the real system is applying. The result is expected to observe is completely different from the other obtained in the previous model. In fact, the only forces that act onto the platform are those applied by cables, which are not sufficient to satisfy the entire motion of the end-effector, i.e. the motion of the belt won't be the same because the subject is not reacting with any wrench to the cable forces.

Looking at the model in figure 4.8 it is possible to understand that it is different from the other one described in the previous subsection: first, in correspondence to the anchor points that should be coiled around the motor's drum, the cable continues to go down until it meets a ball where it is attached to. This ball (with negligible inertia) is constrained to slide on a prismatic joint direct along the Global Reference Frame  $z$  axis, letting it slide freely in that direction while applying a force along the cable. The figure 4.9 shows the detail of the ball hung to the cable, which has been routed onto another pulley in order to keep it straight like in the real tests.

The rest of the model is the same as the one described in the previous subsection,

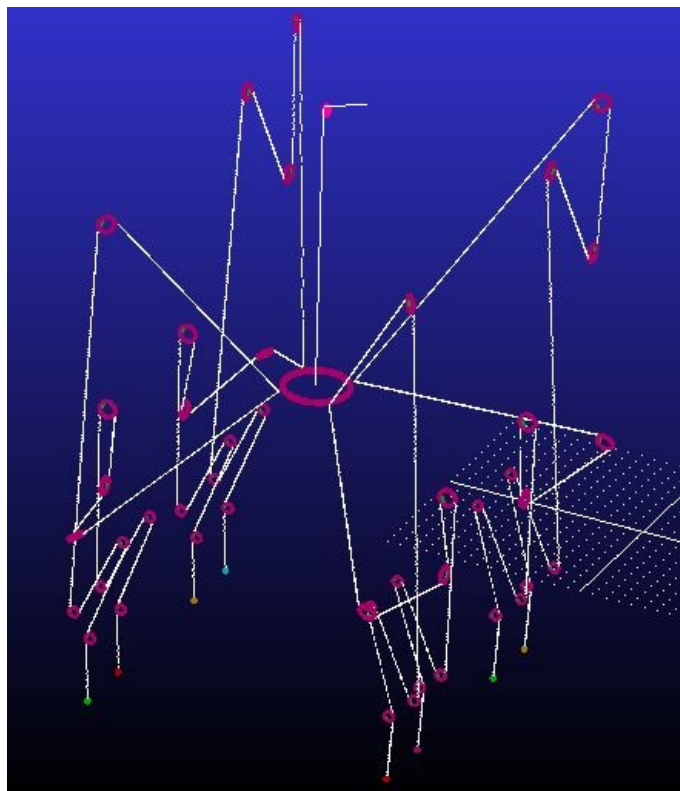


Figure 4.8: Stand Trainer Model: "Model 2".

but this time there was no need to create winch nor state variables because the cable tension was imposed by just applying a force along the negative Global Reference  $z$  direction, generating a curve of points, like in the previous model, and join them with a cubic fitting spline sampled at 200 Hz (one point every 0.005 millisecond).

Another important part that is needed to underline is that differently from the

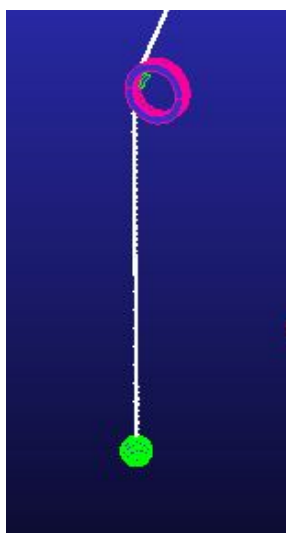


Figure 4.9: Ball hung to the cable - Model 2.

real robot, this virtual model needs a 9th cable coming down from the upper part and to be attached to the belt COM. Contrary, the belt would fall down because of the weight of the subject, since it is bigger than the force the cables are applying to

move it. In fact, the robot can not apply this big amount of force able to completely lift a body from the ground, i.e. it can not generate a force equals to the total body-weight of the person, therefore the belt would sure fall on the ground whether this 9th cable wasn't implemented.

The use of this 9th cable makes the system different to the other described in the previous section, where the motors are actuated. In fact, in this way the obtained results are not comparable with the other two models, but it will be possible just to make some considerations with respect to the real system behavior.

The addition of this new cable makes another consideration coming up: the body where the cable force is being applied is acting like a dead body, as it was pointed out at the beginning of the chapter. Therefore, the dynamic behavior of the system won't be the same, as predicted at the beginning, because the subject is not applying any resistance to the motion. In other words, the subject is not applying any external wrench to the belt.

#### 4.2.2.1 Model 2 Outputs

When analyzing the results that one can obtain with this model, it comes up right away that the dynamic behavior of the mechanism can not be the same that it has in the real world. As far as the cables tensions are concerned, it is possible to have an overview of their accuracy in figure 4.10, where the plots overlap each others and the tensions are correct, since they had been already imposed before.

By considering the geometry of the system also correct, the wrench the cables apply to the end-effector is the same that they apply during the real test.

The problem that comes up with this model is that, as pointed out before, the dynamics are not the same. In fact, the motion that comes out it's completely different to the one recorded from the real test, because the body is not reacting to the wrench that the cables are applying on it and its inertia is providing a much slower motion, completely different to the one recorded. This, at first glance, strange behavior is depicted in figure 4.11, where the Global coordinates  $x$ ,  $y$ ,  $z$  are plotted and compared with the recorded ones. This is the reason why this model can not be considered as a good model able to simulate the real behavior, even though the cable tensions are consistent with the real one.

That is the moment to develop a third model that will join the two previous ones, in order to build a valid system that can be representative of the real robot, with the same motion of the belt COM and the same cables tensions.

### 4.2.3 Model 3: application of the cable tensions and the motion to the belt COM

After having taken a look to the previous two models and their incompatibilities that occur while trying to simulate the real system behavior, it is time for the third and last model developed using Adams environment. While in the first one the motors velocities and in the second one cable tensions were imposed, in this model it has been decided to apply the cables tensions like it was done in the previous one, since the wrench generated by cables is consistent with the real robot, and the motion to the belt, with respect to the Global Reference Frame(a motion on the belt COM along the three directions  $x$ ,  $y$  and  $z$  is imposed). This motion was recorded with

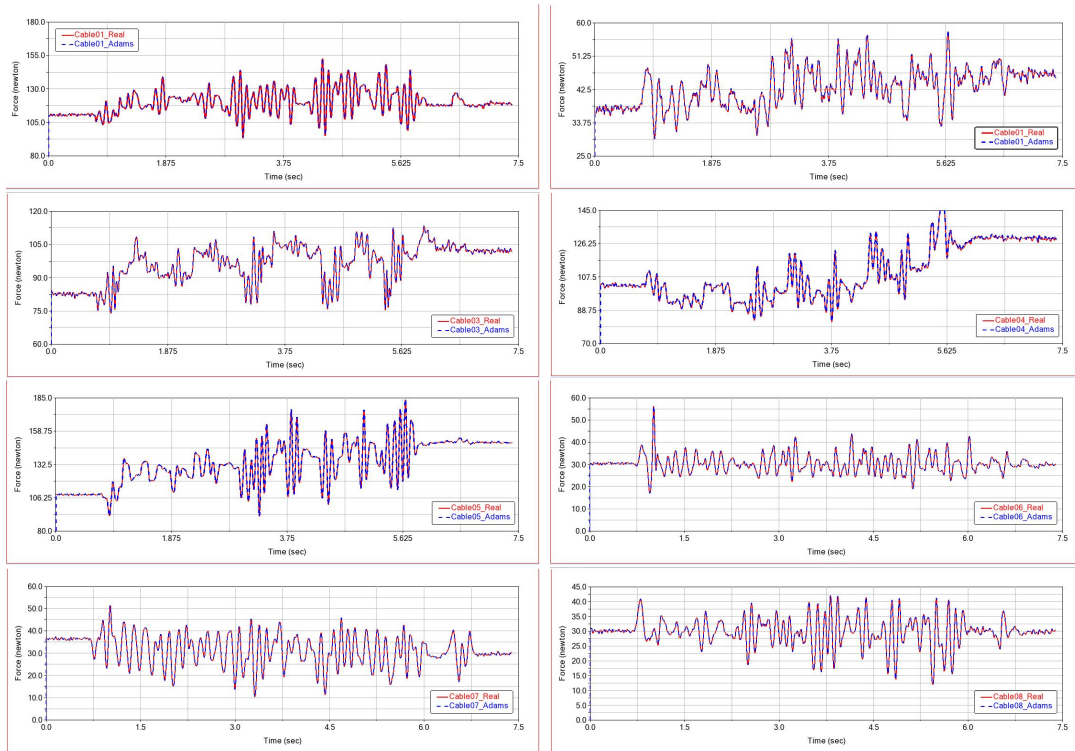


Figure 4.10: Cables Tensions - Model 2.

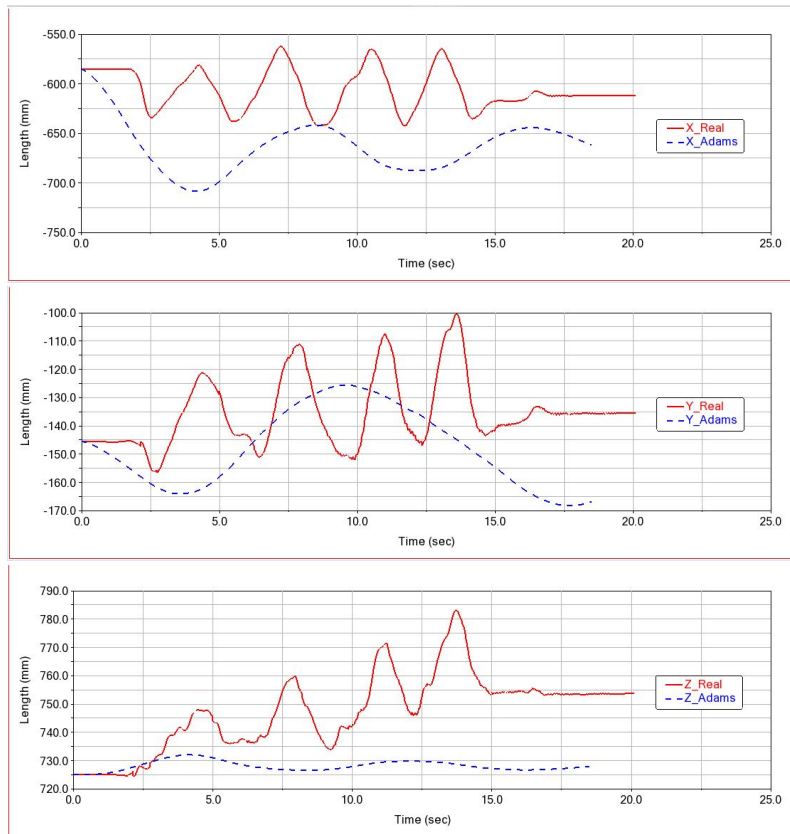


Figure 4.11: Belt Cartesian Position Comparison - Model 2.

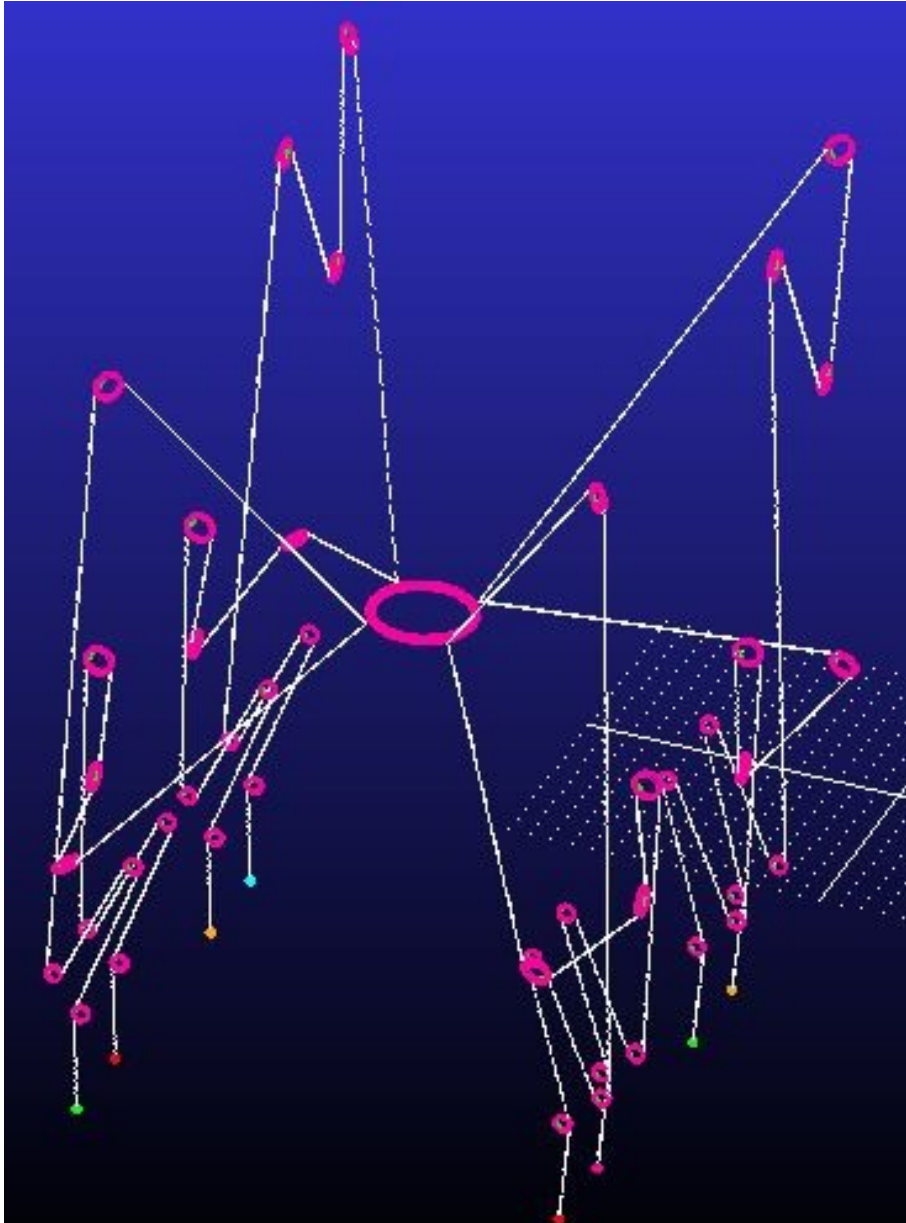


Figure 4.12: Stand Trainer Model: "Model 3".

the Vicon Cameras during the tests on the real system.

Figure 4.12 gives an overview of the system in the Adams environment, where one can notice that there is no more the cable that avoid the belt falling down, because now the body won't result passive to the cable forces, but its behavior will be the same as the ones recorded during the real tests, since the motion to the belt COM is imposed. It is also important to underline that the anchor points (side of the frame) are still attached to the spheres hung to the lower part of the cables, in order to be able to apply tensions to the cables during the simulation.

The consequence is that the body has the same twist and the same twist rate of change of the real one, that means the same inertia wrench applied on the body.

This also means that the choice of the best model that can better replay the real system behavior is set on the Model 3. The motion of the belt COM and cable tensions are exactly the same compared to the real system, since they were previously imposed. The consideration that comes up from this concepts is that the best model that can replay the real behavior of the robot needs either motion of the belt and cable tensions to work properly, while the other models described before can't be considered totally correct for the aim of this thesis, showing several problems.

After that, it is possible to start the activity of post-processing by analyzing the results and looking for some interesting points. In fact, the aim of this thesis is to find the wrench that the human body exerts during the test for every time instance, in order to resist the cable forces applied on it. This could be very useful from a rehabilitative point of view and to set some rehabilitation training sessions, because by knowing the wrench that a healthy subject can apply, it is possible to recognize right away whether a patient has some particular diseases. Also it can be useful to identify where these diseases are located, in terms of what muscle area, by decomposing the wrench in different directions. By observing the amount of force that a certain muscle applies, it will be possible to know better what the working muscles are and how much are they forcing (with or without the help of EMG analysis). In the first case just making some suppositions, in the second, one can have the certainty whether that particular muscle is working or not. For a better discussion of the results, the conclusions chapter will give more informations about the points that came up with this analysis.

### 4.3 Post-Processing and Results

After all the tests on the Stand Trainer and the simulations ran on its Adams model, it is necessary to describe what are the results and the considerations that it is possible to deduce, comparing the models and going beyond.

In the previous section the Stand Trainer models have been built, described and discussed, finding that the Model 3, where cable tensions and motion of the platform are applied, is the one that better replay the behavior of the real robot. Since this consideration holds true, all the post-processing analysis will be carried out using this model.

### 4.3.1 Force Control in Rehabilitation

The first important consideration coming up after the description of the models and their outputs is that in rehabilitation applications, where people are subject to the work of the robot, a force control to the robot is needed. In fact, the user is supposed to apply a target force in relation to the height and/or the weight of the person, age, disease, etc... Since this concerns a rehabilitation activity, he/she will support this wrench applied by the robot, while his/her movement will follow as consequence. The motion of the motors will follow as consequence too, in order to reach those cable tensions which generate that particular wrench previously imposed, preceding the motion of the subject.

If a motion control was applied on the robot, the target of the system would be a final position of the end-effector (the human body), that would mean impose a position or a velocity to the motors, no matter how much the cable tensions and then the wrench applied to the end-effector are. Since this holds true and as it has been possible to observe in the Model 1, the subject who wears the belt and is controlled by the robot would get injured, because of the extremely high values of the wrench applied on him/her, no matter he/she is healthy or not.

This result validates the idea, already put in practice, of using a force control for the Stand Trainer applications and in the most of the cases regarding rehabilitation robotics. These simulations show that it is justified and it is mandatory to use a type of control like this because of the huge wrench that a position control would apply on the subject under rehabilitation.

### 4.3.2 Post-Processing of the Model

Since the more accurate model between the different three is the third, because it better replay the real behavior, the post-processing activity will take into account just this one. Only its outputs will be post-processed and it will be possible to discuss some interesting considerations after its analysis.

The final aim of this post-processing activity will be finding the wrench that the subject of the experiment is applying, by means of the dynamic equations of the system, considering the weight of the person and his/her inertia. The knowledge of this data will be useful for some considerations which the chapter about the conclusions will discuss.

The dynamic equation of a CDPR, as seen in the first chapter, can be written in this way:

- *Translation:*

$$m\ddot{\mathbf{i}} = \mathbf{f}_{\text{sub}} + \mathbf{f}_{\text{cable}} \quad (4.1)$$

- *Rotation:*

$$\mathbf{I}\dot{\boldsymbol{\omega}} + \boldsymbol{\omega} \times (\mathbf{I}\boldsymbol{\omega}) = \boldsymbol{\tau}_{\text{sub}} + \boldsymbol{\tau}_{\text{cable}} \quad (4.2)$$

where

$$\begin{bmatrix} \mathbf{f}_{\text{cable}} \\ \tau_{\text{cable}} \end{bmatrix} = \mathbf{w}_{\text{cable}} \quad (4.3)$$

$$\mathbf{w}_{\text{cable}} = \mathbf{A}^T \mathbf{t} \quad (4.4)$$

$$\begin{bmatrix} \mathbf{f}_{\text{sub}} \\ \tau_{\text{sub}} \end{bmatrix} = \mathbf{w}_{\text{sub}} \quad (4.5)$$

with

$m$ : mass of the human body;

$\mathbf{A}$ : Jacobian matrix of the system ( $6 \times 8$ );

$\mathbf{t}$ : vector of cables tensions ( $8 \times 1$ );

$\mathbf{I}$ : inertia matrix of the human body ( $3 \times 3$ );

$\omega$ : COM angular velocity ( $3 \times 1$ );

$\dot{\omega}$ : COM angular acceleration ( $3 \times 1$ );

$\ddot{\mathbf{r}}$ : COM linear acceleration ( $3 \times 1$ );

$\mathbf{f}_{\text{sub}}$ : force that the subject applies on the system ( $3 \times 1$ );

$\mathbf{f}_{\text{cable}}$ : force that the cables apply on the belt COM ( $3 \times 1$ );

$\tau_{\text{sub}}$ : torque that the subject applies on the system ( $3 \times 1$ );

$\tau_{\text{cable}}$ : torque that the cables apply on the belt COM ( $3 \times 1$ );

$\mathbf{w}_{\text{sub}}$ : wrench that the subject applies on the system ( $6 \times 1$ );

$\mathbf{w}_{\text{cable}}$ : wrench that the cables apply on the belt COM ( $6 \times 1$ );

Finally, is it possible to join the two equations systems into one, knowing that:

$$\mathbf{M} = \begin{bmatrix} m\mathbf{E} & \mathbf{0} \\ \mathbf{0} & \mathbf{I} \end{bmatrix} \quad (4.6)$$

$$\ddot{\mathbf{x}} = \begin{bmatrix} \ddot{\mathbf{r}} \\ \dot{\omega} \end{bmatrix} \quad (4.7)$$

$$\mathbf{g} = \begin{bmatrix} 0 \\ 0 \\ -g \\ 0 \\ 0 \\ 0 \end{bmatrix} \quad (4.8)$$

$$\begin{bmatrix} \mathbf{0} \\ \omega \times (\mathbf{I}\omega) \end{bmatrix} = \mathbf{a} \quad (4.9)$$



It is therefore known the dynamic equation that governs the physics of the system under analysis:

$$\mathbf{M}\ddot{\mathbf{x}} + \mathbf{a} - \mathbf{w}_{\text{sub}} - m\mathbf{g} = \mathbf{w}_{\text{cable}} \quad (4.10)$$

with  $g$ : acceleration of gravity = 9.806 m/s<sup>2</sup>;

$\mathbf{M}$ : mass matrix ( $6 \times 6$ );

$\ddot{\mathbf{x}}$ : COM acceleration ( $6 \times 1$ );

$\mathbf{E}$ : identity matrix ( $3 \times 3$ );

In the following paragraph all these terms seen in the equations above and how to take them out of the analyzed Stand Trainer model will be discussed.

First of all, it is necessary to know what is the wrench acting on the belt COM, generated by cables, since the tensions are well known being an input. For this aim, Adams allows the user to compute the total forces acting in a certain location while there are different forces applied on it. This is the case of the belt anchor points, where for each one there are two cables pulling on it. Since the segments that join two opposite anchors in the  $xy$ -plane cross in the belt COM, and since it occurs also in the other two planes ( $xz$ ,  $yz$ ), the system can be considered as symmetric with respect to that point. Therefore the forces resultant is the sum of the resultants in every anchor, for every direction of the Global Reference Frame. By carrying out the sum for each component of every force acting on every anchor, it's possible to obtain the resultant of the forces acting on the belt COM applied by cables. In figure 4.13 it's shown the total force acting on the belt COM after having carried out the sum of every component of every resultant force on each anchor applied by cables. These three components plotted on the figure form the vector  $f_{\text{cable}}$  introduced in the equations above. At first glance, the data collected seem to be very noisy and not consistent because of some force peaks that seem inexplicable because too high to be applied on a subject. These peaks are actually due to the fact that the system is over-constrained, because, as explained in the first chapter where theoretical issues are discussed, it owns 8 cables for 6 DOFs of the belt, when for controlling the end-effector 7 cables are enough to have those degrees of freedom. Since the system is over-constrained, in order to move between two different positions, and since the belt is modelled as a rigid body, the cable tensions peaks represent a physic consequence of the problem, which translate in forces peaks on the belt. Moreover, they're summed with some numerical errors that can occur during the integration of the simulation provided by the software. This effect needs to be somehow filtered during the post-processing stage, in order to read acceptable data without any noise or disturbance, but taking also into account that some unusual peaks need to exists (even if in less magnitude) because of the mechanics of the system after having introduced all the discussed simplifications.

After having computed  $f_{\text{cable}}$ , it is necessary to know the vector of toques acting onto the belt given by the cables tensions, in order to completely know the components of  $w_{\text{cable}}$ : there will be very tiny values of torques (almost zero), because during the test the aim was to give a certain wrench with a negligible torque and a high force, since that is the interest of the rehabilitation training procedure. Therefore it does make sense having toques values close to zero.

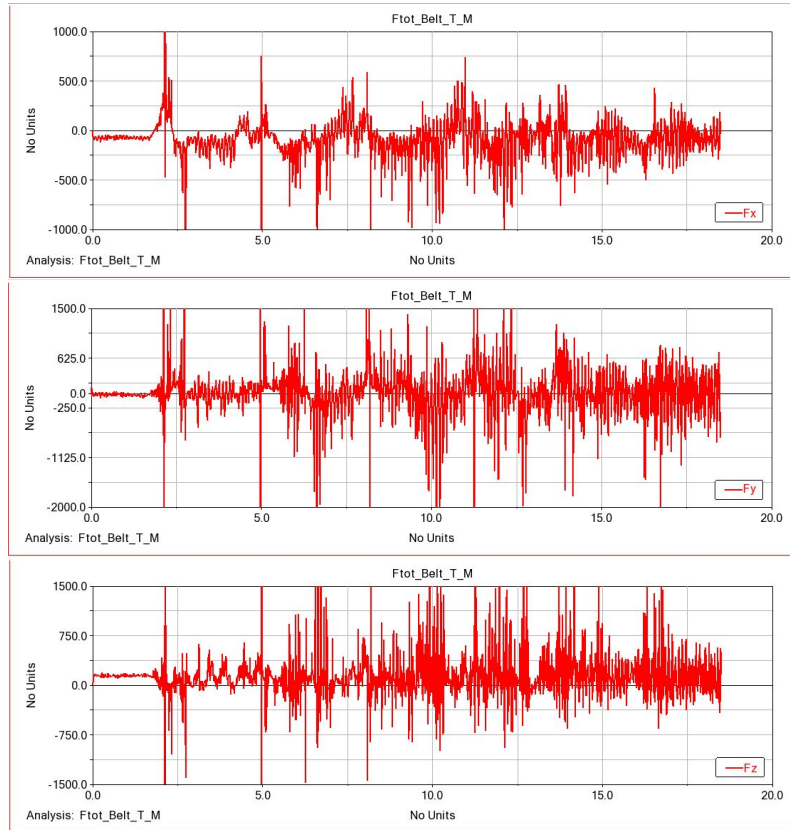


Figure 4.13: Components of the Cartesian forces acting on the belt COM.

The same procedure it was done for the forces acting on the belt COM is supposed to be done for the torques too. The only difference is that for every anchor point of the belt, it's needed to do the cross product between the force vector acting on the  $i$ -th anchor with the position vector that joins the belt COM to it.

$$\tau_{\text{cable}} = \sum_{i=1}^4 \mathbf{f}_i \times (\mathbf{C} - \mathbf{B}_i) \quad (4.11)$$

where

$\mathbf{C}$ : belt COM;

$\mathbf{B}_i$ :  $i$ -th anchor point;

$\mathbf{f}_i$ : force acting on the the  $i$ -th anchor point.

Now that the toques applied by cables are completely known, the total cable wrench is also completely known, therefore from equation 4.10 the wrench applied by the subject wearing the belt can be taken out in a very simple algebraic way, as stated by the following relation:

$$\mathbf{w}_{\text{sub}} = \mathbf{M}\ddot{\mathbf{x}} + \mathbf{a} - \mathbf{w}_{\text{cable}} - m\mathbf{g} \quad (4.12)$$

The goal of computing the wrench applied by the subject during the test is now reached. The next step will be the one of filtering the obtained data on Matlab in order to limit the peaks due to the "infinite" stiffness of the belt moved by an

over-constrained mechanism.

The results are shown in figure 4.14, where it's possible to notice the different force and torque components that the person is applying during the test, called *Rehabilitative Force* and *Torque*. As said before, the data is needed to be filtered and for this aim, a *Butterworth No-Lag* filter was used. Since the human reaction after a force applied on it is about 0.3-0.4 seconds, according to the experience of the ROAR Lab of Columbia University, the biggest frequency is admitted in the wrench that the subject applies is going to be around 2-4 Hz, reason why the cut-off frequency for the filter was set at 3 Hz (that means the reaction that the subject applies is around 0.3 seconds). The sample frequency is set at 200Hz, that is the frequency at which the data acquisition system is also set to.

From the figure one can notice that in general the forces and the torques have

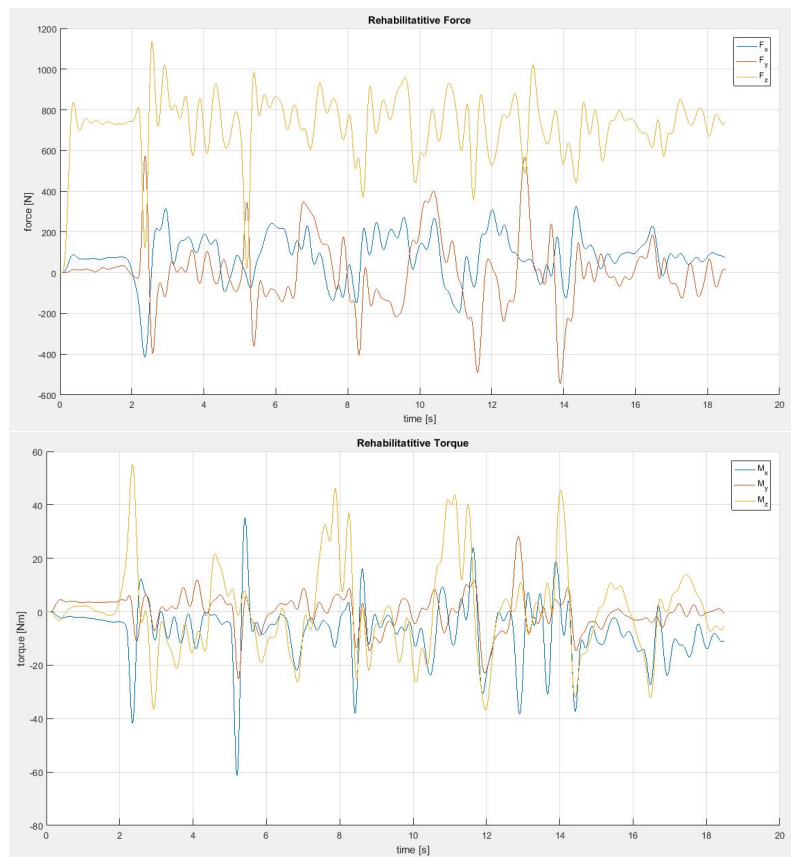


Figure 4.14: Total wrench applied by the subject.

admissible values in terms of the order of magnitude that a person can apply with his/her body, reacting to a force around few hundred of Newtons [26]. Moreover, if one pays attention to the  $z$  component of the force, it's possible to notice that its value is around 8-900 Newtons. Remembering that the body weight of the person was set to 90 kg, it comes out that the reaction force applied by the subject in the  $z$  direction to stay stand on the ground is around 883 Newtons, that let the computed data make some sense.

Another way to see that the computed data make kind of sense is to compute the power provided by the person during the test. It is a trivial operation because it is only needed to multiply the rehabilitative wrench with the COM twist computed by Adams:

$$P = \mathbf{w}_{\text{sub}}^T \dot{\mathbf{x}} \quad (4.13)$$

and the result is shown in figure 4.15.

As one can see, the values are pretty consistent with the power that a person can develop resisting to the forces that the system is applying on him/her [26].

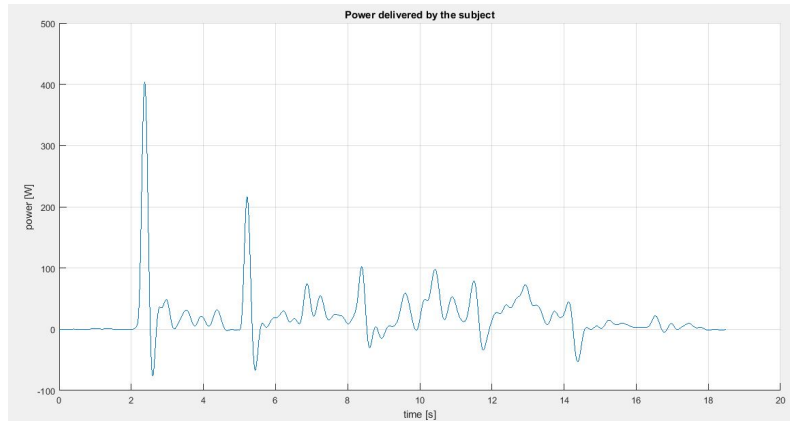


Figure 4.15: Power provided by the subject.

### 4.3.3 Model Limitations

As it's been introduced in the first part of this chapter, the model just described is subject to some simplifications which make it not perfectly exact with respect to the real system, but at the same time it can be simple to obtain very powerful results. It is important to underline some limitations of the model in order to think about new developments in the future regarding its setup.

The first limitation that comes up, because it is directly related with the results, is that the belt is a rigid body, with an infinite stiffness that causes high values of cable tensions, leading to high values of the wrench applied to the body. Moreover, in the dynamic equation no elastic forces acting on the system appear, being consistent with the model built. Other forces are not considered in this equation, for example the friction forces on the pulleys, which cause a variation of tensions along the cables, and the damping forces applied first by the belt and then by the human body. Anyway, even though it can be complex to build a model that takes these effects into account, there is always the possibility to add some springs to the cables in order to lessen the problem of the high cable tensions when moving from a position to another. For instance, the springs could replace the final part of the cable that is attached to belt, replaying its elasticity even though the body is set as rigid. Adams gives also the possibility to build a spring-damper system all together, like a shock absorber. It could be interesting because the results would be similar to the ones the real model gives, but at the same time the dynamic equation 4.10 would be much more complex to be modelled.

Another important limitation is that the mass of the body is supposed to be concentrated in its COM, that is not true at all, causing a different behavior compared to the real one. In order to improve this aspect, a model of the human body can

be introduced and it can replace the only belt which in that case would be lighter and more similar to the real one. Doing this, also the inertia of the system would be more accurate and more similar to the real one, while in the current model it has been built from experimental results, neglecting the non-diagonal terms.

The last improvement that can be added is the passage from the *Simplified* method of integration to the *Discretized* one, described at the beginning of the chapter: in this way the gravitational and inertial effects of the cables can be taken into account, having a more precise system.

Anyway, after the description of all these limitations, if the most precise model was wanted to be built, there could be some drawbacks that can cause a lot of efforts to reach the goal, finding only at the end that all these efforts were not worth it enough, because the improvement of the obtained results wouldn't be so high as the efforts have been made would be. Eventually, improving the model is always good, but also keeping it as simple as possible is always a very good approach, being aware of the simplifications and approximations made.

After having built the three models just described in this chapter, having set the simulations and extracted the results on which it was possible to apply post-processing work, something feasible to carry out would be the analysis of these results in order to set a proper work of training for people with different kinds of muscles diseases, observing their improvement after every training session. Moreover, it can be possible to notice what is the force patients have more problems to develop, and with the help of EMG signals coming from their muscles, it can be feasible to identify their problems and work on them.



# Chapter 5

## Conclusions

This thesis addresses several aspects about a new cable-driven parallel robot developed for rehabilitation application at Columbia University ROAR Lab. In particular, the core of this study concerns the dynamic model of the Stand Trainer, a CDPR with 8 cables built for rehabilitation applications.

Its model was built on Adams, by introducing several simplification shown in the chapter 4 in order to limit computational load.

The following considerations are addressed either to the obtained results and to possible future works. Outputs of the model and their analysis in the post-processing activity are commented, by showing the characteristics that can be improved in order to reach more accuracy. Moreover, possible future developments are discussed, by explaining the utility of the model during a rehabilitative training session.

### 5.1 Discussion of the Results

The three models that have been built in Adams, described in the last chapter, underlined several differences that made one of them behave better than the others. The Model 1, where motors velocities are imposed, is considered good in terms of motion replaying of the end-effector, but since the cable tensions are too high for the aim of rehabilitation robotics, that lead to a too high wrench applied onto the body COM, it is not considered a good model for the simulation of the real system behavior.

In the Model 2, where cable tensions are imposed, the exact cable wrench is exerted onto the subject, but since the motion of the end-effector is completely different from the real one (the subject is acting as a dead body), this model can not be considered good for the simulation of the real behavior. Moreover it was necessary to add another cable in order to avoid the person falling down, since the force applied by cables are not enough to totally lift a person. This element makes the system not comparable with the other two if one wanted to do a comparison between the models, because this new cable represents another constraint that changes the system configuration.

Eventually, the Model 3 has been considered the best, since the belt COM trajectory and cable tensions are imposed based on the real data previously recorded. Therefore its behavior can be considered very similar to the real one and its study is allowed.

For this aim, with the help of Adams again, it was possible to analyze more in de-

tail the obtained results after having run the simulation. In particular, it has been possible to compute the wrench the subject was exerting during the test by just applying the dynamic equations of motion.

Clearly, even though it is the most accurate between the three, this model shows several limitations that make the results not totally true. Because of this, their analysis must be carried out by considering these limitations and by interpreting the obtained results paying particular attention to the differences that can occur in the real behavior.

In fact, figures 4.14 show that the wrench applied by the subject seem to have too high peaks that a person hardly exerts compared to the amount of cable forces that was applied during the test. This is due to the absence of elasticity and dumping in the belt, modelled as a rigid body which is over-constrained by the cables. Moreover, the wrench exerted by the subject, computed with the equation of motion, must be applied by different muscles positioned in different areas of its body, but in this model, all the forces and torques coming from the subject are exerted as if all the muscles were concentrated in the body COM.

## 5.2 Future Developments

The use of a simulation model able to well replay the real system behavior can be beneficial for several aspects. This is the reason why its development, in terms of accuracy with respect to the real system, is important.

Next steps that can be taken in order to move forward and find more accurate results are different:

- Build a new model whose geometry is exactly the same as the one of the real device, without considering the system symmetric with respect to the saggital plane;
- Add the elasticity to the belt, which can take into account either the one of the belt and the one of the subject. This can be useful to avoid the noisy behavior seen in figure 4.13 and have a more consistent result as far as the rehabilitative wrench is concerned (figure 4.14). By considering the belt elasticity, the model would become more complex in terms of computational load. A solution for this problem can be the addition of springs in correspondence with the anchor points of the belt: it consists in replacing the final part of each cable with a spring and connecting it to the belt. Every one will be characterized by a certain stiffness, equivalent to the one that the system "belt-human body" has;
- The same considerations can be pointed out when taking into account the damping: by adding the springs as described in the previous point, Adams allows to add also a damping coefficient to them. In this way, the final part of each cable will present a shock absorber before reaching the belt, with the equivalent stiffness and damping coefficient that the system "belt-human body" has;
- Add a human body model to the system, having a specific mass and inertia different for every patient. Building and applying this model can be complex,



because human body has a lot of DOFs that need lot of computational efforts to be simulated and implemented in a system like the one that this thesis discusses.

- In order to have a more complete model, it is necessary to have the possibility to let the subject take a step during the tests, which usually occurs because sometimes the force is high and the person falls out from his/her limits of stability;
- Add mass to the cables, considering the gravitational effects and their inertia while they are pulled. This can be done by implementing the *Discretized Method* that Adams offers in order to model cables.

All these considerations regards the Adams model which is supposed to replay the behavior of the real system, and they can be necessary to make the simulation model better.

As far as practical applications are concerned, the analysis that this thesis shows lays the basis for the development of a new tool which can be used during training sessions for patients. It is now possible to understand what the patient under training is doing, i.e. what forces he/she is exerting. This can be useful in order to understand if and how much the patient is improving his/her muscle activation, by observing the results obtained by the dynamic analysis (like the ones shown in figure 4.14) after every training session.

Therefore, this tool can represent a new way, combined with EMG signals, to analyze the improvement of a patient that is underwent to a rehabilitative treatment.

In conclusion, this thesis shows how it's possible to compute the wrench that a patient exerts during a training session for his/her rehabilitation using a 8-CDPR, by applying the dynamic equation of motion to the system and with the help of a simulation software like Adams where its virtual model has been built. Some limitations of this model have been outlined, but also some considerations to make it better have been explained.

The main result that is possible to outline with the help of this thesis is that by using the Adams model in combination with EMG data, it will be possible to observe the increase of patients' muscle activation day by day, being also able to understand if the training suggested is useful or not.



# Bibliography

- [1] M. Arsenault. “Stiffness analysis of a planar 2-dof cable-suspended mechanism while considering cable mass”. In: *Cable-Driven Parallel Robots*. Springer, 2013, pp. 405–421.
- [2] H. Barbeau and S. Rossignol. “Recovery of locomotion after chronic spinalization in the adult cat”. In: *Brain research* 412.1 (1987), pp. 84–95.
- [3] T. Bruckmann et al. “Wire robots part I: Kinematics, analysis & design”. In: *Parallel Manipulators, New Developments*. InTech, 2008.
- [4] G. Castelli and E. Ottaviano. “Modelling, simulation and testing of a reconfigurable cable-based parallel manipulator as motion aiding system”. In: *Applied Bionics and Biomechanics* 7.4 (2010), pp. 253–268.
- [5] X. Cui et al. “Design of a 7-DOF Cable-Driven Arm Exoskeleton (CAREX-7) and a Controller for Dexterous Motion Training or Assistance”. In: *IEEE/ASME Transactions on Mechatronics* 22.1 (Feb. 2017), pp. 161–172. ISSN: 1083-4435. DOI: 10.1109/TMECH.2016.2618888.
- [6] C. J. De Luca. “The use of surface electromyography in biomechanics”. In: *Journal of applied biomechanics* 13.2 (1997), pp. 135–163.
- [7] W. Erdmann. “Geometry and inertia of the human body - review of research”. English. In: *Acta of Bioengineering and Biomechanics* Vol. 1, nr 1 (1999), pp. 23–35.
- [8] M. Frey et al. “A novel mechatronic body weight support system”. In: *IEEE Transactions on Neural Systems and Rehabilitation Engineering* 14.3 (2006), pp. 311–321.
- [9] C. Gosselin. “Cable-driven parallel mechanisms: state of the art and perspectives”. In: *Mechanical Engineering Reviews* 1.1 (2014), DSM0004–DSM0004.
- [10] R. Hidayah et al. “Comparing the Performance of a Cable-Driven Active Leg Exoskeleton (C-ALEX) Over-Ground and on a Treadmill”. In: *2018 7th IEEE International Conference on Biomedical Robotics and Biomechanics (Biorob)*. IEEE. 2018, pp. 299–304.
- [11] X. Jin, X. Cui, and S. K. Agrawal. “Design of a cable-driven active leg exoskeleton (C-ALEX) and gait training experiments with human subjects”. In: *2015 IEEE International Conference on Robotics and Automation (ICRA)*. May 2015, pp. 5578–5583. DOI: 10.1109/ICRA.2015.7139979.
- [12] M. I. Khan et al. “Enhancing seated stability using trunk support trainer (TruST)”. In: *IEEE Robotics and Automation Letters* 2.3 (2017), pp. 1609–1616.

- [13] M. Khan, V. Santamaria, and S. Agrawal. “Improving Trunk-Pelvis Stability Using Active Force Control at the Trunk and Passive Resistance at the Pelvis”. In: *IEEE Robotics and Automation Letters* (2018).
  - [14] K. Kozak, Q. Zhou, and J. Wang. “Static analysis of cable-driven manipulators with non-negligible cable mass”. In: *IEEE Transactions on Robotics* 22.3 (2006), pp. 425–433.
  - [15] P. de Leva. “Adjustments to Zatsiorsky-Seluyanov’s segment inertia parameters”. In: *Journal of Biomechanics* 29.9 (1996), pp. 1223–1230. ISSN: 0021-9290. DOI: [https://doi.org/10.1016/0021-9290\(95\)00178-6](https://doi.org/10.1016/0021-9290(95)00178-6). URL: <http://www.sciencedirect.com/science/article/pii/0021929095001786>.
  - [16] Y. Mao and S. K. Agrawal. “Design of a Cable-Driven Arm Exoskeleton (CAREX) for Neural Rehabilitation”. In: *IEEE Transactions on Robotics* 28.4 (Aug. 2012), pp. 922–931. ISSN: 1552-3098. DOI: 10.1109/TR0.2012.2189496.
  - [17] Y. Mao et al. “Human Movement Training With a Cable Driven ARm EXoskeleton (CAREX)”. In: *IEEE Transactions on Neural Systems and Rehabilitation Engineering* 23.1 (Jan. 2015), pp. 84–92. ISSN: 1534-4320. DOI: 10.1109/TNSRE.2014.2329018.
  - [18] MSC. *Adams Help*.
  - [19] E. Ottaviano. “A system for tension monitoring in cable-based parallel architectures”. In: *Proceedings of the 12th IFToMM World Congress, Besançon, France*. Vol. 6. 2007.
  - [20] A. Pott. *Cable-Driven Parallel Robots: Theory and Application*. Vol. 120. Springer, 2018.
  - [21] A. Rodriguez-Barroso et al. “Cable-Driven Parallel Robot with Reconfigurable End Effector Controlled with a Compliant Actuator”. In: *Sensors* 18.9 (2018), p. 2765.
  - [22] D. Sui et al. “Design of a wearable upper-limb exoskeleton for activities assistance of daily living”. In: *Advanced Intelligent Mechatronics (AIM), 2017 IEEE International Conference on*. IEEE. 2017, pp. 845–850.
  - [23] D. Surdilovic and R. Bernhardt. “STRING-MAN: a new wire robot for gait rehabilitation”. In: *IEEE International Conference on Robotics and Automation, 2004. Proceedings. ICRA’04. 2004*. Vol. 2. IEEE. 2004, pp. 2031–2036.
  - [24] D. Surdilovic, J. Zhang, and R. Bernhardt. “STRING-MAN: Wire-robot technology for safe, flexible and human-friendly gait rehabilitation”. In: *2007 IEEE 10th International Conference on Rehabilitation Robotics*. IEEE. 2007, pp. 446–453.
  - [25] V. Vashista, M. Khan, and S. K. Agrawal. “A novel approach to apply gait synchronized external forces on the pelvis using A-TPAD to reduce walking effort”. In: *IEEE robotics and automation letters* 1.2 (2016), pp. 1118–1124.
  - [26] D. A. Winter. *Biomechanics and motor control of human movement*. John Wiley & Sons, 2009.
-